Cell-autonomous targeting of arabinogalactan by host immune factors inhibits mycobacterial growth

Lianhua Qin[a*], Junfang Xu[b*], Jianxia Chen[b*], Sen Wang[c*], Ruijuan Zheng[a], Zhenling Cui[a], Zhonghua Liu[a], Xiangyang Wu[a], Jie Wang[a], Xiaochen Huang[a], Zhaohui Wang[d], Mingqiao Wang[d], Rong Pan[d], Stefan H.E. Kaufmann[e, f, g], Xun Meng[d,h†], Lu Zhang[i†], Wei Sha[j†], Haipeng Liu[k†]

[a] *Shanghai Key Laboratory of Tuberculosis, Shanghai Pulmonary Hospital, Tongji University School of Medicine, Shanghai, China*

[b] *Clinical and Translational Research Center, Shanghai Pulmonary Hospital, Tongji University School of Medicine, Shanghai, China*

[c] *Department of Infectious Diseases, National Medical Centre for Infectious Diseases, National Clinical Research Centre for Aging and Medicine, Shanghai Key Laboratory of Infectious Diseases and Biosafety Emergency Response, Huashan Hospital, Fudan University, Shanghai, China*

[d] *Abmart Inc., Shanghai, China*

[e] *Max Planck Institute for Infection Biology, Berlin, Germany*

[f] *Max Planck Institute for Multidisciplinary Sciences, Göttingen, Germany*

[g] *Hagler Institute for Advanced Study, Texas A&M University, College Station, USA*

[h] *Multitude Therapeutics, Shanghai, China*

[i] *School of Life Science, Fudan University, Shanghai, China*

[j] *Department of Tuberculosis, Shanghai Pulmonary Hospital, Tongji University School of Medicine, Shanghai, China*

[k] *Central Laboratory, Shanghai Pulmonary Hospital, Tongji University School of Medicine, Shanghai, China*

[*] *These authors contributed equally to this work.*

[†] *Correspondence should be addressed to Haipeng Liu (haipengliu@tongji.edu.cn); Wei Sha(shfksw@126.com); Lu Zhang (zhanglu407@fudan.edu.cn) and Xun Meng (xun.meng@ab-mart.com).*

Abstract

Deeper understanding of the crosstalk between host cells and *Mycobacterium tuberculosis* (Mtb) provides crucial guidelines for the rational design of novel intervention strategies against tuberculosis (TB). Mycobacteria possess a unique complex cell wall with arabinogalactan (AG) as critical component. AG has been identified as a virulence factor of Mtb which is recognized by host galectin-9. Here we demonstrate that galectin-9 directly inhibited mycobacterial growth through AG-binding property of carbohydrate-recognition domain 2. Furthermore, IgG antibodies with AG specificity were detected in serum of TB patients. Based on the interaction between galectin-9 and AG, we developed monoclonal antibody (mAb) screening assay and identified AG-specific mAbs which profoundly inhibit Mtb growth. Mechanistically, proteomic profiling and morphological characterizations revealed that AG-specific mAbs regulate AG biosynthesis, thereby inducing cell wall swelling. Thus, direct AG-binding by galectin-9 or antibodies contributes to protection against TB. Our findings pave the way for the rational design of novel immunotherapeutic strategies for TB control.

Keywords

Mycobacterium tuberculosis, tuberculosis, arabinogalactan, galectin-9, antibody

Introduction

Tuberculosis (TB), caused by *Mycobacterium tuberculosi*s (Mtb) remains a considerable threat to human health. In 2021, 10.6 million people fell ill with TB, 1.6 million people died from the disease, and 450,000 new TB cases suffered from rifampicin-resistant or multidrug-resistant TB on this globe [1]. Although TB treatment measures are in place in many parts of the world, cure rates are insufficient due to the increasing emergence of drug resistance. Therefore, novel intervention strategies are urgently needed. Rational design of novel TB therapeutics depends on better understanding of the crosstalk between Mtb and host cells.

Following inhalation of aerosols carrying Mtb, innate immune responses are initiated which constitute a first line of defense. Firstly, Mtb are engulfed by mononuclear phagocytes into the phagosome which matures and then fuses with lysosomes [2]. The pathogen-associated molecular patterns (PAMPs) from Mtb are recognized by a variety of pattern recognition receptors (PRRs), such as Toll-like receptors (TLRs), Nod-like receptors (NLRs), C-type lectins receptors (CLRs) and cyclic GMP-AMP synthase (cGAS), resulting in production of inflammatory cytokines, chemokines and anti-bacterial peptides to restrict bacterial growth [3-6]. Mtb can escape from the phagosome into the cytosol and can be recaptured in autophagosomes, through a process termed xenophagy, to form a degradative autolysosome [7,8]. Cell-autonomous defense mechanisms also include production of reactive oxygen and nitrogen intermediates, hypoxia, mild acidity and nutrition deprivation [9,10]. These mechanisms help to limit growth and spread of the bacteria

within the cell, and contribute to the initiation of an adaptive immune response. However, our knowledge about host immune factors that target Mtb components and directly inhibit replication is limited.

Mtb can evade and resist immune defense by entering a state of dormancy which can last for years. This is due to the capacity of Mtb to synthesize a sturdy cell wall, slow down metabolism to promote growth arrest and implement the so-called stringent response [11,12]. These mechanisms provide the basis for long-term persistence of Mtb until immune control weakens. Once immune control deteriorates, Mtb acquires a metabolic active stage and induces progression to active TB.

The complex cell wall of Mtb provides a barrier not only for host defense, but also for antibiotics. Accordingly, components of the cell wall are well-established drug targets. The essential core cell wall structure is composed of three distinct layers: a) the cross-linked network of peptidoglycan (PGN), b) the highly branched arabinogalactan (AG) polysaccharide, and c) the characteristic long-chain mycolic acids [13]. Among these, AG has been an important target for anti-TB drugs, though understanding of its biological functions is limited. E.g., ethambutol, one of the front-line anti-TB drugs, targets the arabinosyltransferases EmbA, EmbB and EmbC, which are critical for AG synthesis [14-16]. However, it remains unclear whether AG is directly targeted by natural host immune factors in TB.

Recently, we identified AG as a virulence factor of Mtb that is recognized by galectin-9, a member of the β-galactoside binding gene family. Upon AG binding, galectin-9 initiates the downstream TAK1-ERK-MMP signaling cascade leading to

pathologic impairment of the lung [17]. Galectin-4 and galectin-8 directly kill *E.coli* by recognizing blood group antigens of bacteria [18]. This raises the question whether galectin-9 inhibits mycobacterial growth via targeting AG. Here, we demonstrate a novel cell-autonomous mechanism by which galectin-9 impedes mycobacterial growth via its AG-binding property in a carbohydrate recognition domain (CRD) 2-dependent mode. Moreover, in sera of TB patients, we identified anti-AG IgG antibodies which were supposed to defend against TB. Employing a monoclonal antibody (mAb) screening array, we identified anti-AG mAbs, CL010746 and CL046999, which were capable of restraining Mtb growth by regulating AG biosynthesis. Thus, AG possesses characteristic features of protective antigens. In sum, our work identified a previously unknown role of galectin-9 and anti-AG antibodies in TB control. Hence, our findings provide the basis for rational design of mAb-based immunotherapy of TB as a novel approach towards host-directed therapy of one of the deadliest infectious diseases globally.

Results

Galectin-9 inhibits mycobacterial growth

Our previous work demonstrated that galectin-9 directly interacts with AG and AG-containing bacteria [17]. Given the capacity of galectin-4 and galectin-8 to kill *E.coli* [18], we interrogated whether galectin-9 directly interferes with mycobacterial replication. Real-time monitoring of *in vitro* cultures revealed that recombinant galectin-9 protein inhibits growth of Mtb at a concentration as low as 10 ng/mL **(Figure 1A)**. Native structural conformation of galectin-9 was required for its bacteriostatic effect since heat inactivation at 95 □ for 5 min abrogated this activity **(Figure 1B)**. CFU assays further validated that galectin-9 inhibited Mtb growth **(Figure 1C)**. Galectin-9 also impaired replication of the fast-growing *Mycobacterium smegmatis* in a dose-dependent manner **(Figure 1D)**. Consistently, ELISA revealed profoundly higher abundance of galectin-9 in serum from TB patients than that from heathy donors, implying that galectin-9 contributes to resistance against Mtb infection **(Figure 1E)**. Of note, average concentration of galectin-9 in sera of healthy donors was 3.602 ng/mL **(Figure 1E)**. We speculate that this high abundance of galectin-9 contributes to maintenance of latent TB infection by restricting Mtb spreading from granuloma, where the pathogen is contained. In sum, we conclude that galectin-9 directly inhibits mycobacterial growth.

Macrophages are part of the first line defense against invading mycobacteria. When human monocytic THP-1 cells were infected with *Mycobacterium bovis* BCG fused with DsRed, immunofluorescence assays revealed recruitment of galectin-9 to

mycobacteria in a time-dependent manner **(Figure 1F and 1G)**. In line with this observation, robust accumulation of galectin-9 around invading Mtb H37Rv-GFP was also observed in THP-1 cells post infection **(Figure 1H and 1I)**. Though galectin-9 has been reported to be critical for initiation of mTOR signaling and induction of autophagy [19-21], our work revealed a novel cell-autonomous mechanism whereby galectin-9 recruitment restricts mycobacterial growth in an autophagy-independent manner.

Carbohydrate recognition is essential for galectin-9-mediated inhibition of mycobacterial growth

Given that galectin-9 binds to β-galactoside, we interrogated whether carbohydrate recognition by galectin-9 is essential for inhibition of mycobacterial growth. Addition of lactose rich in β-galactoside (generally used for neutralization of carbohydrate binding of galectin-9) completely reversed mycobacterial growth inhibition by galectin-9 *in vitro* **(Figure 2A)**. In contrast, addition of glucose had no such effect **(Figure 2B)**. These results indicate that the β-galactose binding property of galectin-9 is involved in mycobacterial activity. Moreover, addition of AG reversed growth inhibition by galectin-9 **(Figure 2C)**, indicating that the AG-binding property of galectin-9 is involved in anti-mycobacterial activity. Our previous work had demonstrated that CRD2, but not CRD1, of galectin-9 mediated its interaction with AG [17]. As expected, addition of purified CRD2, but not of CRD1, to some extent hindered Mtb growth, emphasizing that AG binding to galectin-9 was sufficient for

anti-mycobacterial effects **(Figure 2D)**. aken together, carbohydrate recognition is essential for galectin-9-mediated inhibition of mycobacterial growth.

Identification of anti-AG antibodies from TB patients

Given the higher abundance of galectin-9 in serum from active TB patients, we next interrogated whether anti-AG antibodies are present in serum of TB patients. An ELISA assay was developed for identification of anti-AG antibodies by coating AG on plates **(Figure 3A)**. An adequate window of serum dilutions allowed a linear correlation between OD_{450} and dilution over an appropriate range **(Figure 3B)**. Subsequently, we determined the relative abundance of anti-AG serum antibodies in 17 healthy donors and 25 active TB patients, all of whom had received BCG vaccination within 24 hours after birth. Our findings revealed a significant increase in the abundance of anti-AG antibodies among TB patients when compared to healthy donors **(Figure 3C)**. We speculate that during Mtb infection, anti-AG IgG antibodies are induced, which potentially contribute to protection against TB by directly inhibiting Mtb replication albeit seemingly in vain. Whether anti-AG antibody levels at site of Mtb growth in patients are too low or whether growth inhibition is nullified by excessive replication of Mtb remains to be solved in the future.

Generation of anti-AG mAb

Based on the finding that AG binding of galectin-9 inhibits mycobacterial growth, we embarked on the development of anti-AG mAbs with blocking acivity. Given the high affinity between galectin-9 and AG, we developed an antibody chip comprising

62,208 mAbs to screen for anti-AG activity [17]. Briefly, the antibody chip was incubated with AG, and bound AG was subsequently detected using galectin-9 in conjunction with FITC-labeled anti-galectin-9 monoclonal antibody **(Figure 4A)**. We filtered out 12 candidate mAbs exhibiting binding affinity to AG **(Figure 4A, B)**. Subsequently, we validated their AG-binding capacity using ELISA. AG was coated on plates, and mAbs were added in 2-fold serial dilutions **(Figure 4C)**. The ELISA assay revealed a robust AG-binding curve for CL010746 (referred to as mAb1) and CL046999 (referred to as mAb2) **(Figure 4D)**. Furthermore, both mAbs exhibited specific binding to Mtb H37Rv-GFP as demonstrated by immunofluorescent assay **(Figure 4E, F**). Therefore, we have successfully developed anti-AG mAbs that bind Mtb directly.

Anti-AG antibody inhibits Mtb growth

For functional characterization, we monitored the *in vitro* mycobacterial growth in the presence or absence of anti-AG mAbs. Both mAb1 and mAb2 demonstrated inhibition of Mtb growth **(Figure 5A)**. This finding was further confirmed through CFU determination **(Figure 5B)**. Likewise, both mAbs markedly inhibited growth of *Mycobacterium smegmatis* as evidenced by real-time OD monitoring **(Figure 5C)** and CFU assay **(Figure 5D)**. In conclusion, the newly identified anti-AG mAbs demonstrated direct blockade of mycobacterial growth through binding to AG. Direct inhibitory effects on Mtb growth by anti-AG antibodies emphasize that AG expresses features of protective antigens.

Proteomics profiling of the mycobacterial response to anti-AG mAb

To elucidate the molecular mechanisms underlying inhibition of mycobacterial growth by anti-AG antibodies, we conducted proteomic profiling of Mtb in response to anti-AG mAb1 treatment. Gene ontology (GO) enrichment analysis revealed significant enrichment of numerous cellular and metabolic processes, primarily related to biosynthesis of outer membrane, upon treatment with anti-AG mAb1. These processes include cell periphery, external encapsulating structure, organic substance metabolic process, cellular metabolic process, primary metabolic process, nitrogen compound metabolic process, and biosynthetic process (**Figure 6A**). Moreover, the formamidopyrimidine-DNA glycosylase N-terminal domain was enriched based on the analysis of functional enrichment and protein domain of differentially expressed antigens **(Figure 6B, C)**. Additionally, the KEGG pathway analysis demonstrated a significant enrichment of lipoarabinomannan (LAM) biosynthesis pathways **(Figure 6D)**. Consistently, the upregulated proteins Rv0236.1 and Rv3806c were involved in the biosynthesis of the mycobacterial cell wall arabinan **(Figure 6E)**. In the re-annotated genome sequence of Mtb, Rv0236.1 consists of Rv0236c and Rv0236A. Rv0236c is predicted to be a cognate of the GT-C superfamily of glycosyltransferases and likely acts as arabinofuranosyltransferase involved in AG synthesis [22]. On the other hand, Rv0236A is a small secreted protein involved in cell wall and cell processes [23]. Additionally, Rv3806c is a decaprenylphosphoryl-5-phosphoribose (DPPR) synthase involved in AG synthesis [24]. These data provide compelling

evidence to suggest that anti-AG mAbs regulate AG biosynthesis.

Targeting AG by mAbs modulates the cell wall of Mtb

To verify the impact of anti-AG mAbs on the biosynthesis of the mycobacterial cell wall, we characterized the morphological changes of Mtb treated with or without mAbs. Intriguingly, mAb1 and mAb2 treatment both led to a dispersed distribution of Mtb in cultures (**Figure 7A**). Acid fast staining further revealed the formation of a cord-like structure in Mtb treated with mAb1 or mAb2, which was not observed following ethambutol (EMB) treatment **(Figure 7B)**. Moreover, electron microscopy demonstrated that anti-AG mAbs treatment markedly increased the thickness of the Mtb cell wall **(Figure 7C, D)**. Based on these findings, we conclude that targeting AG by specific antibodies, and likely by galectin-9 as well, impairs growth of Mtb and other mycobacteria by modulating cell wall structure.

Discussion

Mtb, the etiologic agent of TB, is one of the leading causes of death worldwide, further aggravated by increasing incidences of antibiotic resistance [25,26]. Hence, TB remains a major contributor to the global disease burden. Host-directed therapy is increasingly recognized as an alternative or adjunct to antibiotic therapy [27]. Therefore, deeper insights into the interactions between Mtb and the host immune system are warranted. We previously demonstrated that mycobacterial AG binds to the galactoside-binding protein galectin-9, causing pathologic impairments in the lung via

the TAK1-ERK-MMP signaling pathway [17]. Here, we demonstrate that galectin-9 directly impedes mycobacterial growth through its AG-binding property. Further, we identified natural anti-AG antibodies in sera of TB patients, which are predicted to inhibit Mtb growth. Based on these findings, we generated mAbs capable of binding AG and hindering Mtb replication. Proteomics profiling of Mtb revealed that the binding of anti-AG antibodies regulates AG biosynthesis which leads to swelling of the cell wall, as validated by morphological characterization. We conclude that galectin-9 and anti-AG antibodies serve as immune factors that restrain bacterial growth by targeting AG in the cell wall. Increasing evidence suggests a role for antibodies in protection against TB [28,29]. It is generally assumed that the role of antibodies in TB is based on their interactions with macrophages, which promote anti-mycobacterial activities such as phago-lysosome fusion and production of reactive oxygen and nitrogen intermediates [2,9]. In striking contrast, our findings demonstrate that anti-AG antibodies directly impair Mtb growth and thus emphasize that AG comprises features of protective antigens.

Galectins are a highly conserved class of molecules that play critical roles in multiple biological processes. Fifteen different types of galectins are known in humans, which can be classified based on their structure, subcellular localization, and function. For instance, galectin1 participates in regulating cell proliferation, apoptosis, and immune responses through interactions with specific glycosylated receptors on the cell surface, such as integrins and CD45 [30-32]. More recently, it was shown that galectin-4 disrupts bacterial membranes and kills *E.coli* through interactions with

lipopolysaccharides on the bacterial outer membrane [18]. Here, we demonstrate that galectin-9 significantly inhibits replication of Mtb by interacting with AG in Mtb via its CRD2 domain. Similar to galectin-9, galectin-4, galectin-6 and galectin-8 also comprise 2 CRDs in tandem connected by a linker sequence[33]. It remains to be explored whether and how these galectins exert anti-mycobacterial activities via the CRD2 domain, thereby providing general insights into the role of galectin family cognates in immunity to TB.

After phagocytosis by pulmonary macrophages of the newly infected host, Mtb ends up inside phagosomes, where it downregulates its metabolism and enters a non-replicating persistent (NRP) state, termed dormancy, in response to host stress [34,35]. Once the immune response "breaks down", Mtb transits into a metabolically active and replicative state which ultimately results in progression to active TB disease [36].We demonstrated that galectin-9 accumulates around invading mycobacteria in host cells. However, whether Mtb recruit galectin-9 during dormancy, its active stage, or during both stages, has not been investigated. Of note, AG is hidden by mycolic acids in the outer layer. We speculate that during Mtb replication, cell wall synthesis is active and AG becomes exposed, thereby facilitating its binding to galectin-9 and leading to Mtb growth arrest.

Major drugs in clinical use for TB treatment inhibit Mtb growth by targeting different essential components and processes. For instance, Isoniazid inhibits mycolic acid synthesis by targeting InhA enzyme [37], Ethambutol blocks AG biosynthesis by targeting EmbCAB complex [38], and Pyrazinamide disrupts the pH balance within the

bacterial cell, thereby impairing mycobacterial growth [39]. Although the mycobacterial cell wall has been widely exploited as antibiotic target, to date, drugs that directly bind AG and inhibit Mtb growth have not been reported. Here, we identified host galectin-9 and anti-AG antibodies (both serum antibodies from patients and mAbs) which recognize AG and thus inhibit Mtb replication. Hence, anti-AG mAbs can be harnessed for design of novel biologics which address the challenge of drug resistance in TB.

We observed elevated levels of galectin-9 in the serum of active TB patients, consistent with reports indicating that cleaved galectin-9 levels in the serum serve as a biomarker for severe infection [40,41]. We consider that the elevated levels of galectin-9 in the serum of active TB may be an indicator of the host immune response to Mtb infection, however, the magnitude of elevated galectin-9 is not sufficient to control Mtb infection and maintain latent infection. This is highly similar to other protective immune factors such as interferon gamma, which is elevated in active TB as well [42,43]. On the other hand, mechanisms underlying inhibition of mycobacterial growth induced by galectin-9 or anti-AG mAbs remain elusive. We propose they interfere with the activity of enzymes involved in AG biosynthesis and/or modify the physical properties of the cell wall, leading to disruption of AG side chain extension, thereby increasing Mtb vulnerability to host immunity. They may also function through the two-component system, that is commonly found in bacteria and allows bacteria to sense and respond to changes in the environment, such as nutrient availability or stress [44-46]. Interactions between galectin-9 and AG in the cell wall may alter

membrane permeability, which restrains nutrient uptake and activates sensor proteins, causing bacterial growth arrest.

Aside from their direct anti-Mtb activity, anti-AG antibodies in serum of TB patients probably also opsonize Mtb, thereby promoting phagocytosis by mononuclear phagocytes [28,47]. However, the mechanisms by which galectin-9 or antibodies inhibit mycobacterial growth depend on the details of the molecular interactions and require further investigation.

Our knowledge about antibodies which target glycans is scarce, not the least due to technical challenges. Glycan antigens have been identified on the surface of numerous microorganisms and are also expressed by certain cancer cells. Antibodies that recognize and bind these glycan antigens, therefore, are promising candidates for therapy and diagnosis of infectious and malignant diseases. For instance, the mAb 2G12 neutralizes human immunodeficiency virus-1 (HIV-1) by recognizing oligomannose-type N-glycans on the HIV-1 gp120 envelope protein, and the mAb FH6 specifically binds the Sialyl Lewis X (SLeX) antigen on the surface of various cancer cells [48-50]. In this study, we not only discovered anti-AG mAbs which directly impair Mtb growth, but also developed an efficient high-throughput screening for identifying mAbs with specificity for glycans.

In conclusion, we (i) discovered a novel cell-autonomous mechanism by which galectin-9 protects against TB via targeting AG in the cell wall of Mtb, (ii) identified neutralizing antibodies against AG in serum of TB patients, (iii) selected anti-AG mAbs for passive immunization against TB by means of a mAb screening array, (iv)

characterized inhibition of Mtb replication by induction of cell wall swelling as critical mechanism of protection through AG targeting (**Figure 7E**). Our findings, thus, not only provide deeper insights into humoral immune mechanisms involved in protection against TB, but also serve as basis for new intervention strategies against TB in adjunct to chemotherapy.

Materials and Methods

Bacteria

Mtb H37Rv, H37Rv-GFP, *Mycobacterium bovis* BCG, and *Mycobacterium smegmatis* mc^2155, were from Shanghai Key Laboratory of Tuberculosis and grown in Middlebrook 7H9 (Becton Dickinson, Cockeysville, MD) liquid medium supplemented with 0.25% glycerol, 10% oleic acid–albumin-dextrose-catalase (OADC) (Becton Dickinson, Sparks, MD) and 0.05% Tween-80.

In vitro growth of mycobacteria

Mycobacteria were harvested at mid-log phase and diluted to a calculated starting OD600 of 0.25 and added to 96-well culture plates containing Middlebrook 7H9 liquid medium together with antibody or galectin-9. OD600 of each time point of each strain was tested in real time by Bioscreen C microplate incubator (FP1100-C, Labsystems, USA) at 37□.

CFU assay

Mycobacteria were harvested at mid-log phase and diluted to a calculated starting OD600 of 0.25 and incubated in Middlebrook 7H9 liquid medium with or without antibody or galectin-9 for 30 h at 37 □. Appropriate dilutions were plated on 7H10 agar plates for enumeration of CFU.

Immunofluorescence assay

For colocalization of galectin-9 and mycobacteria, immunofluorescence assays were performed as described previously [51]. Briefly, THP-1 cells (ATCC Cat# TIB-202 RRID: CVCL_0006) were infected with bacteria for 2 h, fixed with 4% formaldehyde

for 30 min at R.T., permeabilized with 0.1% Triton X-100 in PBS for 5 min, and blocked with 5% BSA in PBS for 60 min at R.T.. Cells were stained with the anti-galectin-9 antibody (Cell Signaling Technology, Cat#54330, RRID:AB_2799456), antibodies at a dilution of 1:200 in 5% BSA in PBS overnight at 4 °C and then incubated with Alexa Fluor 488 or 555 conjugated secondary antibodies (Thermo Fisher Scientific, Cat# A-11008; RRID: AB_143165; Cat# A32732, RRID:AB_2633281) at a dilution of 1:1000 for 2 h at R.T.. Nuclei were stained with DAPI.

For binding of anti-AG mAb with Mtb, H37Rv-GFP strains were harvested at mid-log phase. Subsequently, 2×10^7 H37Rv-GFP/100 μL FACS buffer was incubated with anti-AG mAb (mAb1 or mAb2, 20 μg/mL) at R.T. for 1h, and washed three times with PBST (PBS containing 0.05 % Tween 20, pH 7.4) by centrifugation (12,000g, 5 min). The resulting sediment was resuspended in 10 μL of ddH2O and smeared on microscopic slides.

Images were acquired using a Leica TCS SP8 confocal laser microscopy system (Leica Microsystems) at ×63 magnification.

Validation of anti-AG antibodies by ELISA

AG antigen (10 μg in 100 μL 0.1 mol/L $NaHCO_3$ buffer, pH 9.4) was added to wells of microwell plates and incubated overnight at 4°C. After four rinses with PBST (PBS containing 0.05 % Tween 20, pH 7.4), the wells were saturated with blocking buffer. After four additional PBST rinses, serum or candidate anti-AG mAbs were added to each well and incubated for 1 h at 37°C. The wells were rinsed three times with PBS

containing 0.05 % Tween 20 and horseradish-peroxidase-labeled rabbit anti-human or anti mouse IgG (100 μL/well; Sigma-Aldrich, Germany) was added to each well and incubated for 1 h at 37°C. Finally, the TMB substrate was added and the absorbance was measured with the Thermo Fisher Scientific Multiskan FC microplate photometer. Clinical serum specimens were collected from 17 healthy volunteers and 25 pulmonary TB patients before undergoing treatment at Shanghai Pulmonary Hospital (Shanghai, PR China), all of whom had received BCG vaccination within 24 h after birth. The donors are between the ages of 50 and 65, ethnic Han, with an equal representation of males and females.

High throughput Screening of anti-AG antibody

Antibody chip harboring 62208 mAbs was incubated with 10 μg AG in 10 mL incubation buffer (1x PBS buffer containing 10% BSA) for 1 h, followed by incubation with 10 μg galectin-9 protein in 10 mL incubation buffer for 1 h. The chip was incubated with rabbit anti-galetin-9 antibody (1:5000 diluted in 10 mL incubation buffer; ab227046, Abcam, UK) followed by staining with FITC-labelled anti-rabbit IgG (1:5000 diluted in 10 mL incubation buffer; ab6717, Abcam, UK). Then the chip was scanned by GenePix 4200A Microarray Scanner (Molecular Devices LLC) and analyzed by GenePix Pro 6.0 software.

Proteomics analysis

LC-MS/MS

Mycobacteria at mid-log phase were diluted to a calculated starting OD600 of 0.25 and incubated in Middlebrook 7H9 liquid medium with or without mAb1 for 30 h at

37 □. The bacterial pellets were collected followed by three washes with sterile saline. The bacterial pellets were resuspended in lysis buffer (8 M urea, 1% Protease Inhibitor Cocktail) and inactivated for 10 min at 100 □. The lysate was sonicated three times on ice using a high intensity ultrasonic processor (Scientz) and centrifuged. The protein concentration of the lysate was determined with BCA kit according to the manufacturer's instructions.

After trypsin digestion, peptides were dissolved in 0.1% formic acid and separated with nanoElute UHPLC system (Bruker, Germany) and subjected to Capillary source followed by the timsTOF Pro mass spectrometry. The resulting MS/MS data were processed using Maxquant search engine (v1.6.6.0). Tandem mass spectra were searched against Mtb strain ATCC 25618 83332 PR 20191210 database (3993 entries) concatenated with reverse decoy database.

Enrichment of Gene Ontology analysis

GO annotations of proteins are divided into three broad categories: Biological Process, Cellular Component, and Molecular Function. For each category, a two-tailed Fisher's exact test was employed to test the enrichment of the differentially expressed protein against all identified proteins. The GO with a corrected p-value < 0.05 was considered significant.

Enrichment of pathway analysis

Kyoto Encyclopedia of Genes and Genomes (KEGG) database was used to identify enriched pathways by a two-tailed Fisher's exact test to test the enrichment of the differentially expressed protein against all identified proteins. The pathway with a

corrected p-value < 0.05 was considered significant. These pathways were classified into hierarchical categories according to the KEGG website.

Enrichment of protein domain analysis

For each category proteins, InterPro database (a resource that provides functional analysis of protein sequences by classifying them into families and predicting the presence of domains and important sites) was researched and a two-tailed Fisher's exact test was employed to test the enrichment of the differentially expressed protein against all identified proteins. Protein domains with a corrected p-value < 0.05 were considered significant.

Morphologic characterization of Mtb

Mtb strains were cultured in 96 U well culture plates containing Middlebrook 7H9 liquid medium with anti-AG antibody or without anti-AG antibody at 37 □, and were grown for 10-14 days until the formation of colonies. Morphologic characterization of tested strains in liquid medium were observed by 2 x magnifier. At the same time, 10 μl of culture were spread onto a glass slide. Smears on glass slides were fixed under ultraviolet light overnight. Glass slides were stained with Ziehl–Neelsen stain using a TB Stain Kit (Baso DIAGNOTICS TAIWAN, Zhuhai, China). Morphological characteristics or cell lengths of tested strains were observed using a Leica DM2500 microscope using the 100× objective.

For ultrastructural characteristics, strains at mid-log phase were collected, and analyzed by Tecnai transmission electron microscopy (TEM) with 160 kV according the procedures of the manufacturer (GOODBIO, Wuhan, China). A 10^7-10^8 bacterial

suspension was used for TEM examination.

Statistical analysis

The statistical significance of comparisons was analyzed with two tailed unpaired Student's t test or Mann-Whitney U test in GraphPad Prism version 8.0.1.. $P < 0.05$ was considered statistically significant. All data are showed as mean ± SD of two or more independent experiments performed in triplicate. Detailed statistical information on each experiment is provided in the respective figure legends.

Acknowledgements

We thank Prof. Baoxue Ge for helpful discussions. This work was supported by the project of National Key R&D Program of China (2021YFA1300902 to R.Z., 2023YFC2307002 to H.L..); the National Natural Science Foundation of China (82271882 to H.L., 82000009 to X.W., 81470090 to L.Q., 82201931 to J.X.,); Science and Technology Commission of Shanghai Municipality (22S11900700 to H.L., 21DZ229800 to H.L., 22ZR1452500 to J.X.); Tongji University Fundamental Research Funds for the Central Universities (22120220655 to J.X.); the National Science Foundation for Excellent Young Scholars of China (81922030); and Shanghai ShuGuang Program (20SG19).

Disclosure Statement

The authors report there are no competing interests to declare.

Author Contributions

H.L. conceived the study and designed the experiments.

L.Q., J.X., J.C., and S.W. analyzed the data and wrote the original draft.

H.L., W.S., L.Z., and X.M. supervised the project and edited the manuscript.

R.Z, Z.C., Z.L., Y.W., J.W., and X.H. performed most of the experiments.

Z.W., M.W., and R.P. performed the bioinformatics analysis.

W.S. provided clinical samples.

S.H.E.K provided helpful discussions and edited the manuscript.

All authors commented on the paper.

Materials availability statement

Bacterial strains and monoantibodies generated in this study are available from the Lead Contact upon reasonable request.

Data availability statement

The authors confirm that the data supporting the findings of this study are available within the article.

Statement of Ethics

This work received approval from the Clinical Ethics Committee of the Shanghai Pulmonary Hospital, which is affiliated with the Tongji University School of Medicine, in accordance with governmental guidelines and institutional policies. Patients providing the pulmonary samples gave informed consent. The ethics committee approved this consent procedure. All protocols were approved by the local ethics committee of Tongji University School of Medicine (permit number: K21-114Y).

References

1. Bagcchi, S. (2023). WHO's Global Tuberculosis Report 2022. Lancet Microbe *4*, e20. 10.1016/S2666-5247(22)00359-7.
2. Chandra, P., Grigsby, S.J., and Philips, J.A. (2022). Immune evasion and provocation by Mycobacterium tuberculosis. Nature reviews. Microbiology *20*, 750-766. 10.1038/s41579-022-00763-4.
3. Reiling, N., Hölscher, C., Fehrenbach, A., Kröger, S., Kirschning, C.J., Goyert, S., and Ehlers, S. (2002). Cutting edge: Toll-like receptor (TLR)2- and TLR4-mediated pathogen recognition in resistance to airborne infection with Mycobacterium tuberculosis. J Immunol *169*, 3480-3484. 10.4049/jimmunol.169.7.3480.
4. Fremond, C.M., Yeremeev, V., Nicolle, D.M., Jacobs, M., Quesniaux, V.F., and Ryffel, B. (2004). Fatal Mycobacterium tuberculosis infection despite adaptive immune response in the absence of MyD88. J Clin Invest *114*, 1790-1799. 10.1172/jci21027.
5. Wilson, G.J., Marakalala, M.J., Hoving, J.C., van Laarhoven, A., Drummond, R.A., Kerscher, B., Keeton, R., van de Vosse, E., Ottenhoff, T.H., Plantinga, T.S., et al. (2015). The C-type lectin receptor CLECSF8/CLEC4D is a key component of anti-mycobacterial immunity. Cell Host Microbe *17*, 252-259. 10.1016/j.chom.2015.01.004.
6. Watson, R.O., Bell, S.L., MacDuff, D.A., Kimmey, J.M., Diner, E.J., Olivas, J., Vance, R.E., Stallings, C.L., Virgin, H.W., and Cox, J.S. (2015). The Cytosolic Sensor cGAS Detects Mycobacterium tuberculosis DNA to Induce Type I Interferons and Activate Autophagy. Cell Host Microbe *17*, 811-819. 10.1016/j.chom.2015.05.004.

512 7. Wang, Z., and Li, C. (2020). Xenophagy in innate immunity: A battle between host and
513 pathogen. Developmental and comparative immunology *109*, 103693.
514 10.1016/j.dci.2020.103693.
515 8. Lopez, A., Fleming, A., and Rubinsztein, D.C. (2018). Seeing is believing: methods to
516 monitor vertebrate autophagy in vivo. Open biology *8*. 10.1098/rsob.180106.
517 9. Nathan, C., and Shiloh, M.U. (2000). Reactive oxygen and nitrogen intermediates in
518 the relationship between mammalian hosts and microbial pathogens. Proc Natl Acad
519 Sci U S A *97*, 8841-8848. 10.1073/pnas.97.16.8841.
520 10. Lupoli, T.J., Vaubourgeix, J., Burns-Huang, K., and Gold, B. (2018). Targeting the
521 Proteostasis Network for Mycobacterial Drug Discovery. ACS infectious diseases *4*,
522 478-498. 10.1021/acsinfecdis.7b00231.
523 11. Batt, S.M., Minnikin, D.E., and Besra, G.S. (2020). The thick waxy coat of
524 mycobacteria, a protective layer against antibiotics and the host's immune system.
525 The Biochemical journal *477*, 1983-2006. 10.1042/bcj20200194.
526 12. Hauryliuk, V., Atkinson, G.C., Murakami, K.S., Tenson, T., and Gerdes, K. (2015).
527 Recent functional insights into the role of (p)ppGpp in bacterial physiology. Nature
528 reviews. Microbiology *13*, 298-309. 10.1038/nrmicro3448.
529 13. Jankute, M., Cox, J.A., Harrison, J., and Besra, G.S. (2015). Assembly of the
530 Mycobacterial Cell Wall. Annu Rev Microbiol *69*, 405-423.
531 10.1146/annurev-micro-091014-104121.
532 14. Escuyer, V.E., Lety, M.A., Torrelles, J.B., Khoo, K.H., Tang, J.B., Rithner, C.D., Frehel,
533 C., McNeil, M.R., Brennan, P.J., and Chatterjee, D. (2001). The role of the embA and

534 embB gene products in the biosynthesis of the terminal hexaarabinofuranosyl motif of
535 Mycobacterium smegmatis arabinogalactan. J Biol Chem *276*, 48854-48862.
536 10.1074/jbc.M102272200.
537 15. Goude, R., Amin, A.G., Chatterjee, D., and Parish, T. (2009). The
538 arabinosyltransferase EmbC is inhibited by ethambutol in Mycobacterium tuberculosis.
539 Antimicrob Agents Chemother *53*, 4138-4146. 10.1128/aac.00162-09.
540 16. Zhang, L., Zhao, Y., Gao, Y., Wu, L., Gao, R., Zhang, Q., Wang, Y., Wu, C., Wu, F.,
541 Gurcha, S.S., et al. (2020). Structures of cell wall arabinosyltransferases with the
542 anti-tuberculosis drug ethambutol. Science *368*, 1211-1219.
543 10.1126/science.aba9102.
544 17. Wu, X., Wu, Y., Zheng, R., Tang, F., Qin, L., Lai, D., Zhang, L., Chen, L., Yan, B.,
545 Yang, H., et al. (2021). Sensing of mycobacterial arabinogalactan by galectin-9
546 exacerbates mycobacterial infection. EMBO reports *22*, e51678.
547 10.15252/embr.202051678.
548 18. Stowell, S.R., Arthur, C.M., Dias-Baruffi, M., Rodrigues, L.C., Gourdine, J.P.,
549 Heimburg-Molinaro, J., Ju, T., Molinaro, R.J., Rivera-Marrero, C., Xia, B., et al. (2010).
550 Innate immune lectins kill bacteria expressing blood group antigen. Nature medicine
551 *16*, 295-301. 10.1038/nm.2103.
552 19. Jia, J., Abudu, Y.P., Claude-Taupin, A., Gu, Y., Kumar, S., Choi, S.W., Peters, R.,
553 Mudd, M.H., Allers, L., Salemi, M., et al. (2018). Galectins Control mTOR in Response
554 to Endomembrane Damage. Mol Cell *70*, 120-135.e128.
555 10.1016/j.molcel.2018.03.009.

556 20. Jia, J., Bissa, B., Brecht, L., Allers, L., Choi, S.W., Gu, Y., Zbinden, M., Burge, M.R.,
557 Timmins, G., Hallows, K., et al. (2020). AMPK, a Regulator of Metabolism and
558 Autophagy, Is Activated by Lysosomal Damage via a Novel Galectin-Directed
559 Ubiquitin Signal Transduction System. Mol Cell *77*, 951-969.e959.
560 10.1016/j.molcel.2019.12.028.
561 21. Bell, S.L., Lopez, K.L., Cox, J.S., Patrick, K.L., and Watson, R.O. (2021). Galectin-8
562 Senses Phagosomal Damage and Recruits Selective Autophagy Adapter TAX1BP1
563 To Control Mycobacterium tuberculosis Infection in Macrophages. mBio *12*, e0187120.
564 10.1128/mBio.01871-20.
565 22. Skovierová, H., Larrouy-Maumus, G., Zhang, J., Kaur, D., Barilone, N., Korduláková,
566 J., Gilleron, M., Guadagnini, S., Belanová, M., Prevost, M.C., et al. (2009). AftD, a
567 novel essential arabinofuranosyltransferase from mycobacteria. Glycobiology *19*,
568 1235-1247. 10.1093/glycob/cwp116.
569 23. Marmiesse, M., Brodin, P., Buchrieser, C., Gutierrez, C., Simoes, N., Vincent, V.,
570 Glaser, P., Cole, S.T., and Brosch, R. (2004). Macro-array and bioinformatic analyses
571 reveal mycobacterial 'core' genes, variation in the ESAT-6 gene family and new
572 phylogenetic markers for the Mycobacterium tuberculosis complex. Microbiology
573 (Reading, England) *150*, 483-496. 10.1099/mic.0.26662-0.
574 24. He, L., Wang, X., Cui, P., Jin, J., Chen, J., Zhang, W., and Zhang, Y. (2015). ubiA
575 (Rv3806c) encoding DPPR synthase involved in cell wall synthesis is associated with
576 ethambutol resistance in Mycobacterium tuberculosis. Tuberculosis *95*, 149-154.
577 https://doi.org/10.1016/j.tube.2014.12.002.

578 25. Singh, V., and Chibale, K. (2021). Strategies to Combat Multi-Drug Resistance in
579 Tuberculosis. Accounts of chemical research *54*, 2361-2376.
580 10.1021/acs.accounts.0c00878.
581 26. Miotto, P., Zhang, Y., Cirillo, D.M., and Yam, W.C. (2018). Drug resistance
582 mechanisms and drug susceptibility testing for tuberculosis. Respirology (Carlton, Vic.)
583 *23*, 1098-1113. 10.1111/resp.13393.
584 27. Kaufmann, S.H.E., Dorhoi, A., Hotchkiss, R.S., and Bartenschlager, R. (2018).
585 Host-directed therapies for bacterial and viral infections. Nature Reviews Drug
586 Discovery *17*, 35-56. 10.1038/nrd.2017.162.
587 28. Lu, L.L., Smith, M.T., Yu, K.K.Q., Luedemann, C., Suscovich, T.J., Grace, P.S., Cain,
588 A., Yu, W.H., McKitrick, T.R., Lauffenburger, D., et al. (2019). IFN-γ-independent
589 immune markers of Mycobacterium tuberculosis exposure. Nature medicine *25*,
590 977-987. 10.1038/s41591-019-0441-3.
591 29. Irvine, E.B., O'Neil, A., Darrah, P.A., Shin, S., Choudhary, A., Li, W., Honnen, W.,
592 Mehra, S., Kaushal, D., Gideon, H.P., et al. (2021). Robust IgM responses following
593 intravenous vaccination with Bacille Calmette-Guérin associate with prevention of
594 Mycobacterium tuberculosis infection in macaques. Nat Immunol *22*, 1515-1523.
595 10.1038/s41590-021-01066-1.
596 30. Cedeno-Laurent, F., Watanabe, R., Teague, J.E., Kupper, T.S., Clark, R.A., and
597 Dimitroff, C.J. (2012). Galectin-1 inhibits the viability, proliferation, and Th1 cytokine
598 production of nonmalignant T cells in patients with leukemic cutaneous T-cell
599 lymphoma. Blood *119*, 3534-3538. 10.1182/blood-2011-12-396457.

600 31. Perillo, N.L., Pace, K.E., Seilhamer, J.J., and Baum, L.G. (1995). Apoptosis of T cells
601 mediated by galectin-1. Nature *378*, 736-739. 10.1038/378736a0.
602 32. Ge, X.N., Ha, S.G., Greenberg, Y.G., Rao, A., Bastan, I., Blidner, A.G., Rao, S.P.,
603 Rabinovich, G.A., and Sriramarao, P. (2016). Regulation of eosinophilia and allergic
604 airway inflammation by the glycan-binding protein galectin-1. Proc Natl Acad Sci U S
605 A *113*, E4837-4846. 10.1073/pnas.1601958113.
606 33. Leffler, H., Carlsson, S., Hedlund, M., Qian, Y., and Poirier, F. (2002). Introduction to
607 galectins. Glycoconjugate journal *19*, 433-440.
608 10.1023/b:Glyc.0000014072.34840.04.
609 34. Russell, D.G. (2001). Mycobacterium tuberculosis: here today, and here tomorrow.
610 Nat Rev Mol Cell Biol *2*, 569-577. 10.1038/35085034.
611 35. Gengenbacher, M., and Kaufmann, S.H. (2012). Mycobacterium tuberculosis: success
612 through dormancy. FEMS microbiology reviews *36*, 514-532.
613 10.1111/j.1574-6976.2012.00331.x.
614 36. van der Wel, N., Hava, D., Houben, D., Fluitsma, D., van Zon, M., Pierson, J., Brenner,
615 M., and Peters, P.J. (2007). M. tuberculosis and M. leprae translocate from the
616 phagolysosome to the cytosol in myeloid cells. Cell *129*, 1287-1298.
617 10.1016/j.cell.2007.05.059.
618 37. Quémard, A., Sacchettini, J.C., Dessen, A., Vilcheze, C., Bittman, R., Jacobs, W.R.,
619 Jr., and Blanchard, J.S. (1995). Enzymatic characterization of the target for isoniazid
620 in Mycobacterium tuberculosis. Biochemistry *34*, 8235-8241. 10.1021/bi00026a004.
621 38. Telenti, A., Philipp, W.J., Sreevatsan, S., Bernasconi, C., Stockbauer, K.E., Wieles, B.,

622 Musser, J.M., and Jacobs, W.R., Jr. (1997). The emb operon, a gene cluster of
623 Mycobacterium tuberculosis involved in resistance to ethambutol. Nat Med *3*, 567-570.
624 10.1038/nm0597-567.
625 39. Zhang, Y., Scorpio, A., Nikaido, H., and Sun, Z. (1999). Role of acid pH and deficient
626 efflux of pyrazinoic acid in unique susceptibility of Mycobacterium tuberculosis to
627 pyrazinamide. Journal of bacteriology *181*, 2044-2049.
628 10.1128/jb.181.7.2044-2049.1999.
629 40. Iwasaki-Hozumi, H., Chagan-Yasutan, H., Ashino, Y., and Hattori, T. (2021). Blood
630 Levels of Galectin-9, an Immuno-Regulating Molecule, Reflect the Severity for the
631 Acute and Chronic Infectious Diseases. Biomolecules *11*. 10.3390/biom11030430.
632 41. Padilla, S.T., Niki, T., Furushima, D., Bai, G., Chagan-Yasutan, H., Telan, E.F.,
633 Tactacan-Abrenica, R.J., Maeda, Y., Solante, R., and Hattori, T. (2020). Plasma
634 Levels of a Cleaved Form of Galectin-9 Are the Most Sensitive Biomarkers of
635 Acquired Immune Deficiency Syndrome and Tuberculosis Coinfection. Biomolecules
636 *10*. 10.3390/biom10111495.
637 42. El-Masry, S., Lotfy, M., Nasif, W.A., El-Kady, I.M., and Al-Badrawy, M. (2007).
638 Elevated serum level of interleukin (IL)-18, interferon (IFN)-gamma and soluble Fas in
639 patients with pulmonary complications in tuberculosis. Acta microbiologica et
640 immunologica Hungarica *54*, 65-77. 10.1556/AMicr.54.2007.1.7.
641 43. Hasan, Z., Jamil, B., Khan, J., Ali, R., Khan, M.A., Nasir, N., Yusuf, M.S., Jamil, S.,
642 Irfan, M., and Hussain, R. (2009). Relationship between circulating levels of
643 IFN-gamma, IL-10, CXCL9 and CCL2 in pulmonary and extrapulmonary tuberculosis

644 is dependent on disease severity. Scandinavian journal of immunology *69*, 259-267.
645 10.1111/j.1365-3083.2008.02217.x.
646 44. Glover, R.T., Kriakov, J., Garforth, S.J., Baughn, A.D., and Jacobs, W.R., Jr. (2007).
647 The two-component regulatory system senX3-regX3 regulates phosphate-dependent
648 gene expression in Mycobacterium smegmatis. Journal of bacteriology *189*,
649 5495-5503. 10.1128/jb.00190-07.
650 45. James, J.N., Hasan, Z.U., Ioerger, T.R., Brown, A.C., Personne, Y., Carroll, P., Ikeh,
651 M., Tilston-Lunel, N.L., Palavecino, C., Sacchettini, J.C., and Parish, T. (2012).
652 Deletion of SenX3-RegX3, a key two-component regulatory system of Mycobacterium
653 smegmatis, results in growth defects under phosphate-limiting conditions.
654 Microbiology (Reading, England) *158*, 2724-2731. 10.1099/mic.0.060319-0.
655 46. Majumdar, S.D., Vashist, A., Dhingra, S., Gupta, R., Singh, A., Challu, V.K.,
656 Ramanathan, V.D., Kumar, P., and Tyagi, J.S. (2012). Appropriate DevR
657 (DosR)-mediated signaling determines transcriptional response, hypoxic viability and
658 virulence of Mycobacterium tuberculosis. PloS one *7*, e35847.
659 10.1371/journal.pone.0035847.
660 47. Chen, T., Blanc, C., Eder, A.Z., Prados-Rosales, R., Souza, A.C., Kim, R.S.,
661 Glatman-Freedman, A., Joe, M., Bai, Y., Lowary, T.L., et al. (2016). Association of
662 Human Antibodies to Arabinomannan With Enhanced Mycobacterial
663 Opsonophagocytosis and Intracellular Growth Reduction. The Journal of infectious
664 diseases *214*, 300-310. 10.1093/infdis/jiw141.
665 48. Trkola, A., Purtscher, M., Muster, T., Ballaun, C., Buchacher, A., Sullivan, N.,

666 Srinivasan, K., Sodroski, J., Moore, J.P., and Katinger, H. (1996). Human monoclonal
667 antibody 2G12 defines a distinctive neutralization epitope on the gp120 glycoprotein of
668 human immunodeficiency virus type 1. J Virol *70*, 1100-1108.
669 10.1128/jvi.70.2.1100-1108.1996.
670 49. Fukushi, Y., Nudelman, E., Levery, S.B., Hakomori, S., and Rauvala, H. (1984). Novel
671 fucolipids accumulating in human adenocarcinoma. III. A hybridoma antibody (FH6)
672 defining a human cancer-associated difucoganglioside (VI3NeuAcV3III3Fuc2nLc6). J
673 Biol Chem *259*, 10511-10517.
674 50. Kannagi, R., Fukushi, Y., Tachikawa, T., Noda, A., Shin, S., Shigeta, K., Hiraiwa, N.,
675 Fukuda, Y., Inamoto, T., Hakomori, S., and et al. (1986). Quantitative and qualitative
676 characterization of human cancer-associated serum glycoprotein antigens expressing
677 fucosyl or sialyl-fucosyl type 2 chain polylactosamine. Cancer research *46*,
678 2619-2626.
679 51. Liu, H., Zhang, H., Wu, X., Ma, D., Wu, J., Wang, L., Jiang, Y., Fei, Y., Zhu, C., Tan, R.,
680 et al. (2018). Nuclear cGAS suppresses DNA repair and promotes tumorigenesis.
681 Nature *563*, 131-136. 10.1038/s41586-018-0629-6.
682
683

Figures

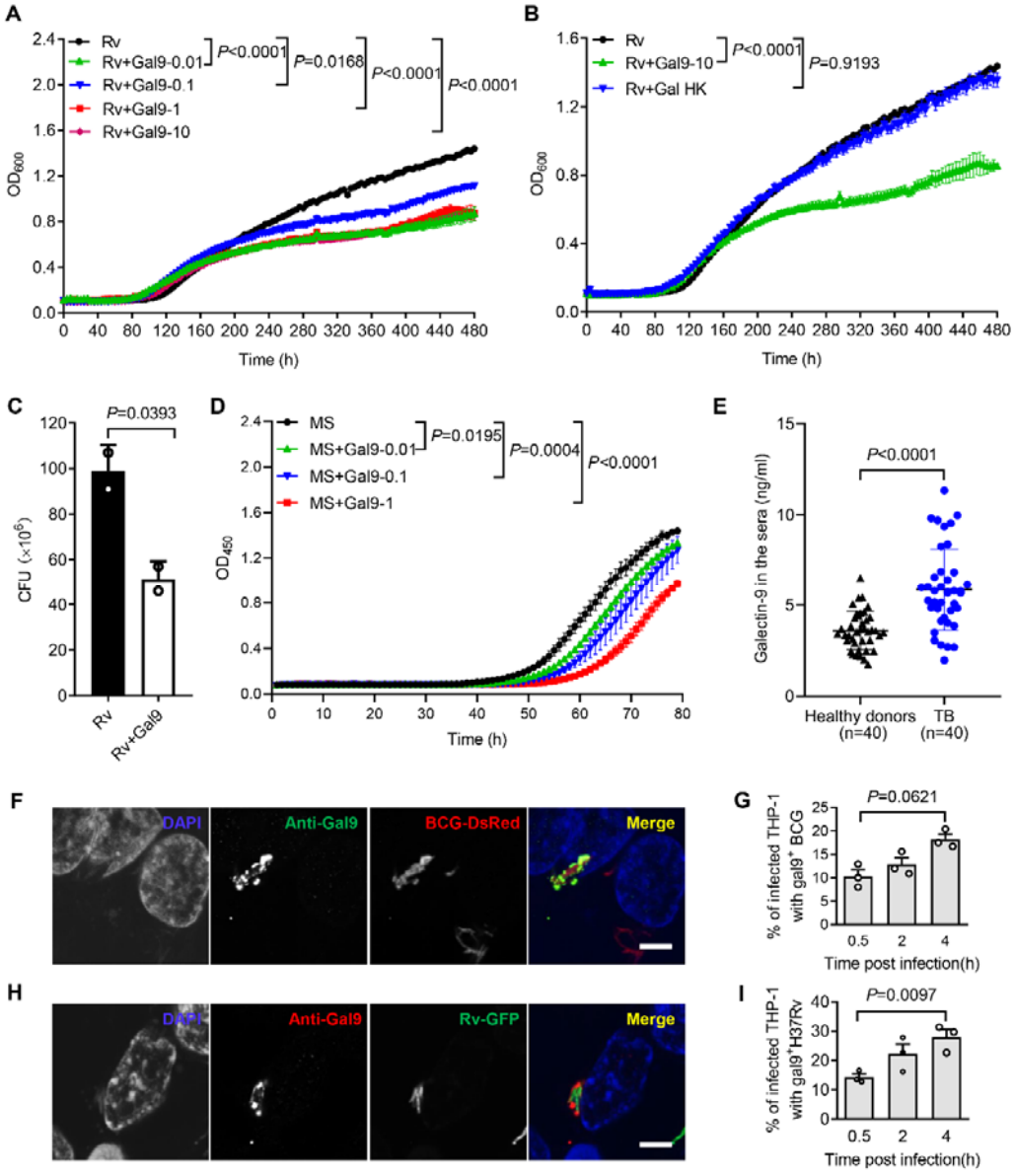

Figure 1. Galectin-9 inhibits mycobacterial growth directly.

A. Profile of Mtb H37Rv (Rv) grown at 37°C in Middlebrook 7H9 liquid medium with different concentration of Galectin-9 (Gal9, 0, 0.01, 0.1, 1, 10 μg/mL). Growth curve was measured using a Bioscreen Growth Curve Instrument. Optical density was measured at absorbance at 600 nm every 2 h.

B. Growth profile of Mtb H37Rv (Rv) in Middlebrook 7H9 liquid medium with10

μg/mL galectin-9 (Gal9) or inactivated galectin-9 (Gal9 HK, heat killed at 95 □ for 5 min).

C. CFU of Mtb H37Rv (Rv) on Middlebrook 7H10 solid medium with or without 10 μg/mL Galectin-9 (Gal9). Cultures were grown at 37°C for 4-8 weeks.

D. Growth profile of *Mycobacterium smegmatis* (MS) in Middlebrook 7H9 liquid medium with different concentrations of Galectin-9 (Gal9, 0, 0.01, 0.1, 1 μg/mL).

E. Concentrations of galectin-9 in sera of healthy donors (n = 40) and active TB patients (n = 40).

F. Confocal microscopy of *M. bovis* BCG-DsRed (BCG-DsRed, red) and Galectin□9 (Anti-Gal9, green) in THP-1 cells. Nuclei was stained with DAPI (blue).

G. Percent of cells with galectin-9 positive ($gal9^+$) BCG in total infected THP-1 cells. Symbols indicate colocalization ratio of at least 12 fields in each experiment.

H. Confocal microscopy of Mtb H37Rv-GFP (Rv-GFP, green) and Galectin□9 (Anti-Gal9, red) in THP-1 cells. Nuclei were stained with DAPI (blue).

I. Percent of cells with galectin9 positive ($gal9^+$) Mtb H37Rv in total infected THP-1 cells. Symbols indicate colocalization ratio of at least 12 fields in each experiment.

Data are shown as mean ± SD, n = 3 biologically independent experiments performed in triplicate (A-D). Data are representative of three independent experiments with similar results (F and H). Two-tailed unpaired Student's t test (A-D, G, and I) or Mann-Whitney U test (E). $P < 0.05$ was considered statistically significant.

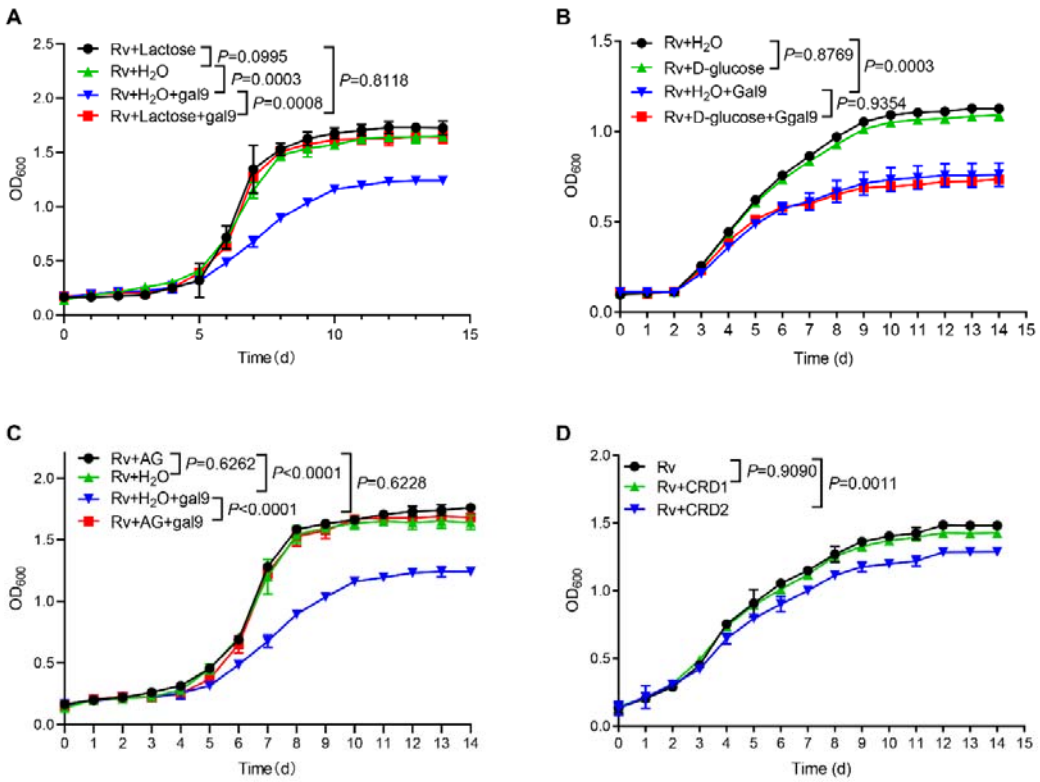

Figure 2. Carbohydrate recognition is essential for galectin-9-mediated inhibition of Mtb growth.

A. Growth profile of Mtb H37Rv (Rv) in Middlebrook 7H9 liquid medium with or without galectin-9 (Gal9, 10 μg/mL) and lactose (1 μg/mL).

B. Growth profile of Mtb H37Rv (Rv) in Middlebrook 7H9 liquid medium with or without galectin-9 (Gal9, 10 μg/mL) and D-glucose (10 μg/mL).

C. Growth profile of Mtb H37Rv (Rv) in Middlebrook 7H9 liquid medium with or without galectin-9 (Gal9, 10 μg/mL) and AG (1 μg/mL).

D. Growth profile of Mtb H37Rv (Rv) in Middlebrook 7H9 liquid medium with 1μg/mL CRD1 or CRD2 of galectin-9.

Data are shown as mean ± SD, n = 3 biologically independent experiments performed in triplicate (A-D). Two-tailed unpaired Student's t test (A-D). $P < 0.05$ was

725 considered statistically significant.

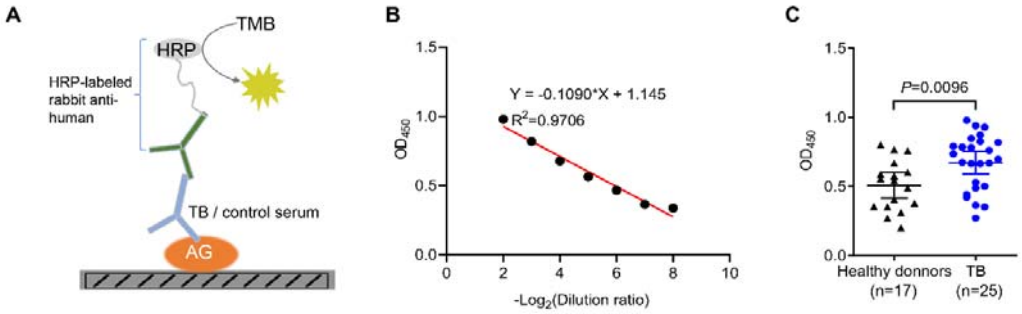

Figure 3. Identification of anti-AG antibodies from TB patients.

A. Schematic presentation of ELISA assay for detecting anti-AG IgG antibodies in the serum of TB patients.

B. Linear correlation between OD and serum dilution ratio determined by ELISA assay.

C. Anti-AG IgG antibodies levels in TB patients (n = 25) and healthy BCG-immunized controls (n = 17) determined via ELISA.

Data are representative of three independent experiments with similar results (B). Mann-Whitney U test (C). $P < 0.05$ was considered statistically significant.

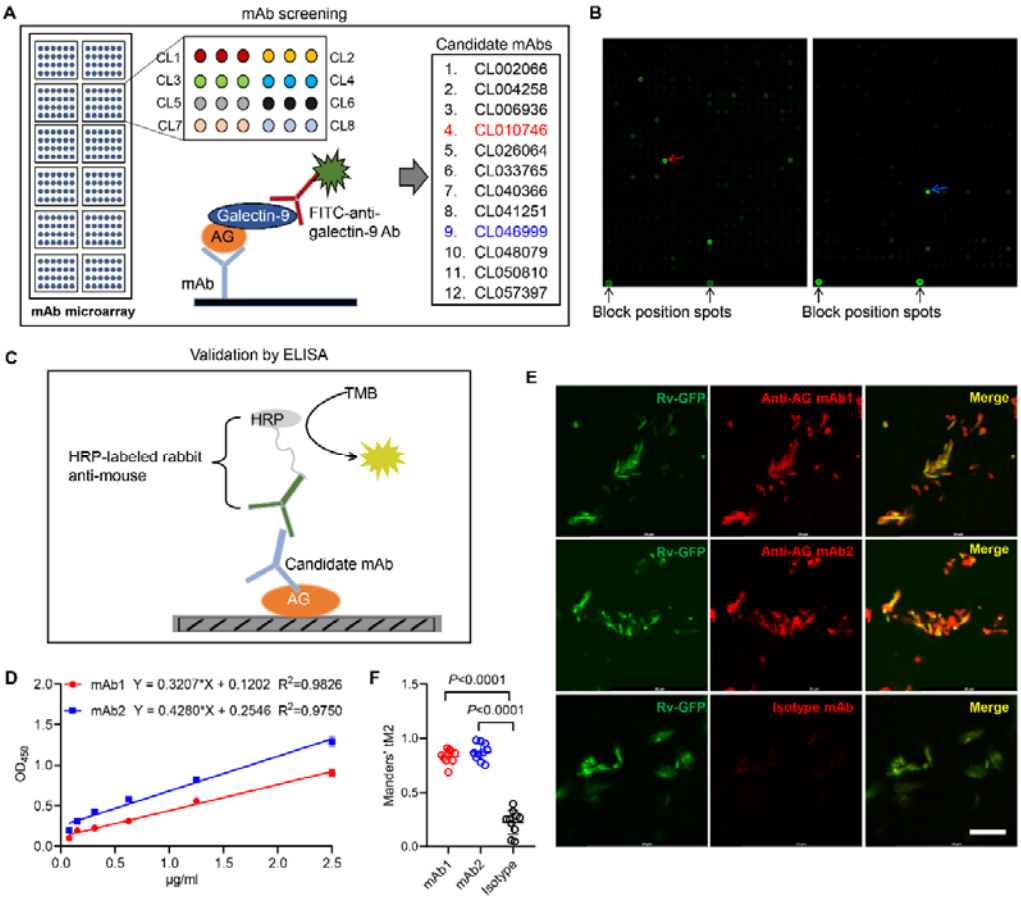

Figure 4. Development of anti-AG mAbs.

A. Schematic presentation of mAb screening for AG specificity.

B. Representative image of chip hybridization for mAb screening. Bright spots in the bottom mark the end line of each array block. Other spots represent AG binding to mAbs. CL010746 (mAb1) and CL046999 (mAb2) were labeled with red arrow and blue arrow, respectively.

C. Schematic presentation of candidate anti-AG mAbs validation by ELISA.

D. Binding curve of mAb1 and mAb2 to AG determined by ELISA assay.

E. Confocal microscopy of Mtb H37Rv-GFP (Rv-GFP, green) and anti-AG mAbs (red).

F. Quantification of colocalization between anti-AG mAb and Mtb H37Rv-GFP by calculating Mander's coefficients in (E). tM2, Mander's coefficient of red above autothreshold of green.

Data are representative of three independent experiments with similar results (D, E). Data are shown as mean ± SD, n = 10 (F). Two-tailed unpaired Student's t test (F). $P < 0.05$ was considered statistically significant.

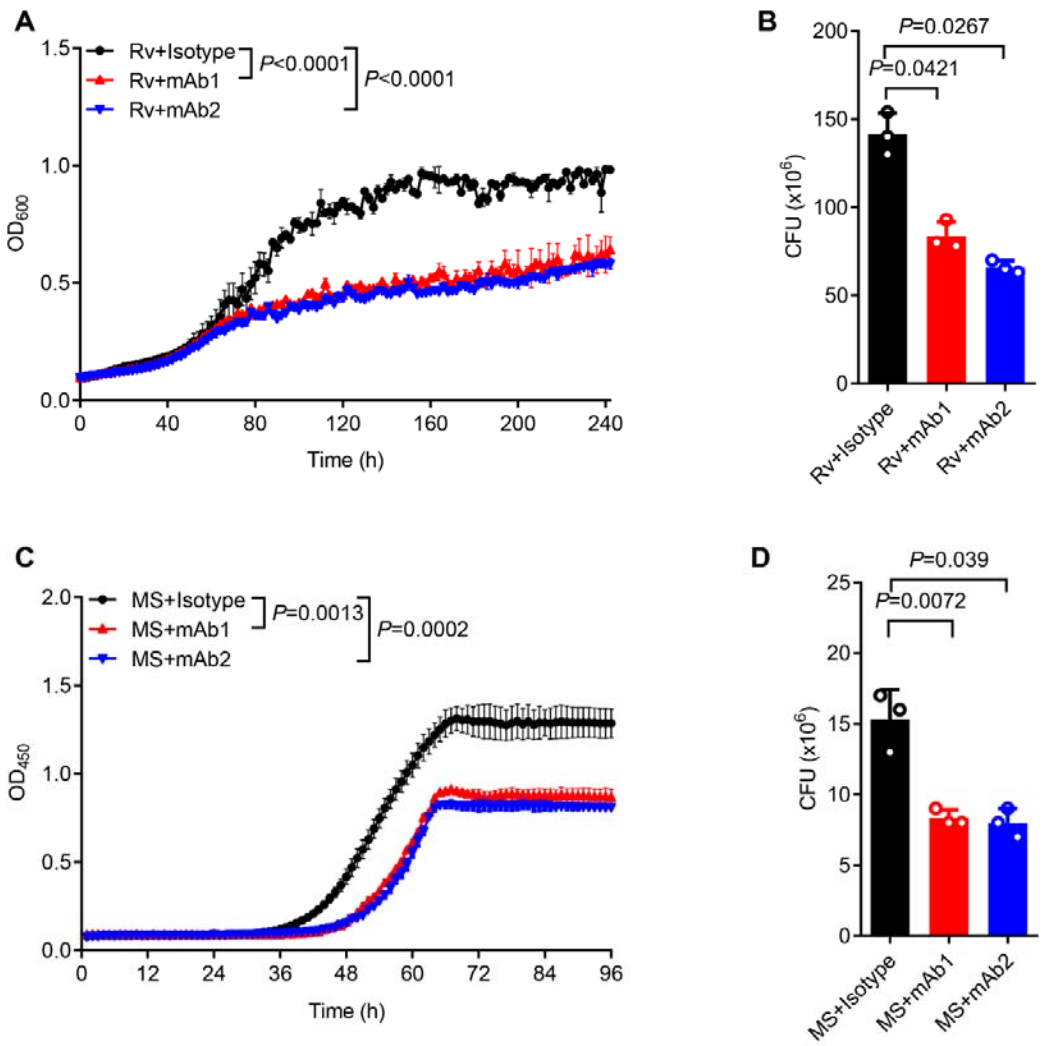

Figure 5. anti-AG antibody inhibits mycobacterial growth.

A. Growth profile of Mtb H37Rv (Rv) in Middlebrook 7H9 liquid medium with or without mAb1/mAb2 (1 μg/mL).

B. CFU of Mtb H37Rv (Rv) on Middlebrook 7H10 solid medium with or without mAb1/mAb2 (1 μg/mL). Cultures were grown at 37°C for 4-8 weeks.

C. Growth profile of *Mycobacterium smegmatis* (MS) in Middlebrook 7H9 liquid medium with or without mAb1/mAb2 (1 μg/mL).

D. CFU of *Mycobacterium smegmatis* (MS) on Middlebrook 7H10 solid medium with or without mAb1/mAb2 (1 μg/mL). Cultures were grown at 37°C for 5-10 days.

Data are shown as mean ± SD, n = 3 (A, C) and n = 3 biologically independent experiments performed in triplicate (B, D). Two-tailed unpaired Student's t test (A-D). $P < 0.05$ was considered statistically significant.

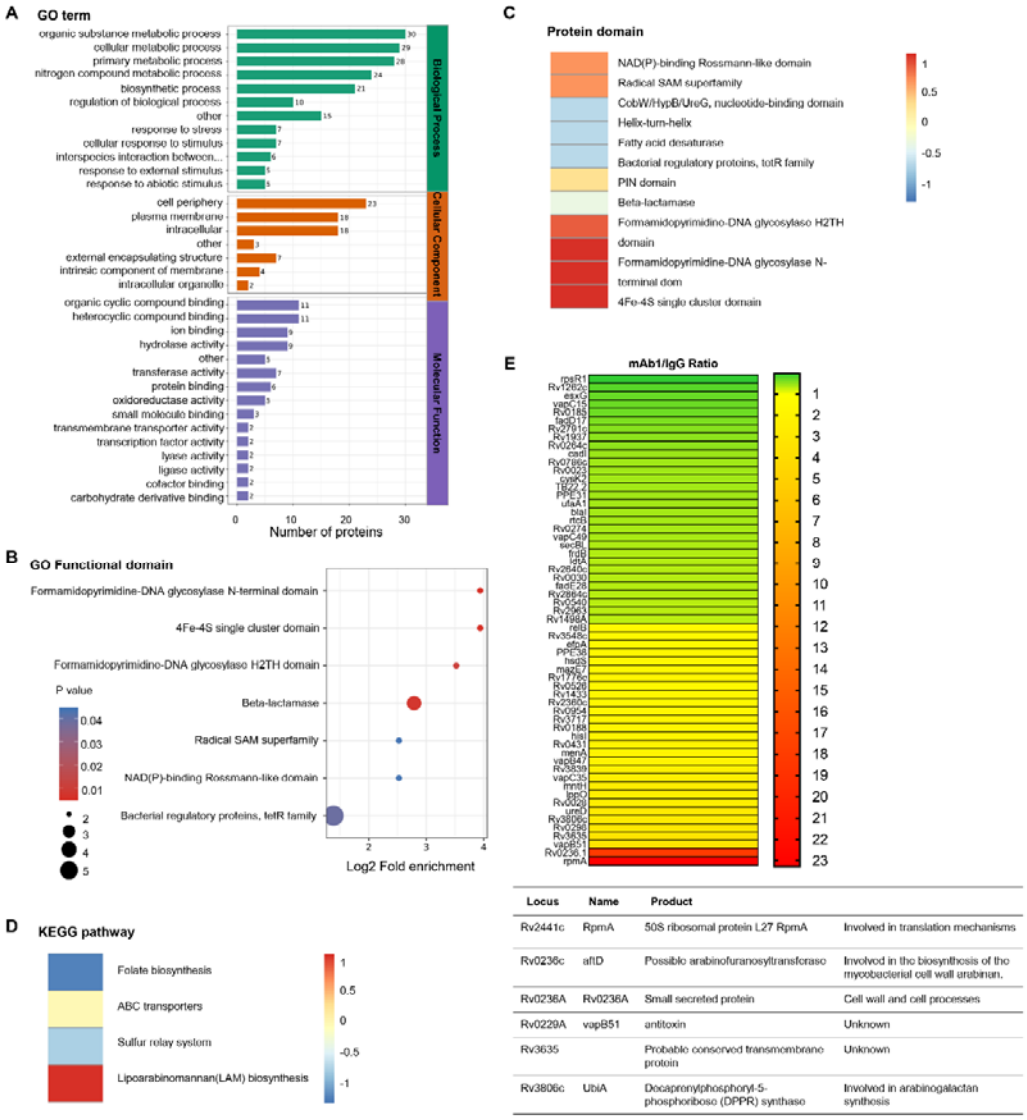

Locus	Name	Product	
Rv2441c	RpmA	50S ribosomal protein L27 RpmA	Involved in translation mechanisms
Rv0236c	aftD	Possible arabinofuranosyltransferase	Involved in the biosynthesis of the mycobacterial cell wall arabinan.
Rv0236A	Rv0236A	Small secreted protein	Cell wall and cell processes
Rv0229A	vapB51	antitoxin	Unknown
Rv3635		Probable conserved transmembrane protein	Unknown
Rv3806c	UbiA	Decaprenylphosphoryl-5-phosphoribose (DPPR) synthase	Involved in arabinogalactan synthesis

Figure 6. Proteomics profiling of the response of Mtb to anti-AG antibody.

A. GO class of differentially expressed proteins in Mtb H37Rv treated with mAb1 (1 μg/mL) for 30 h followed by proteomics analysis. IgG was set as control.

B. Functional enrichment of differentially expressed proteins in Mtb H37Rv in (A).

C. Protein domain of differentially expressed proteins in Mtb H37Rv in (A).

D. KEGG class of differentially expressed proteins in Mtb H37Rv in (A).

E. Upregulation or downregulation genes in Mtb H37Rv in (A).

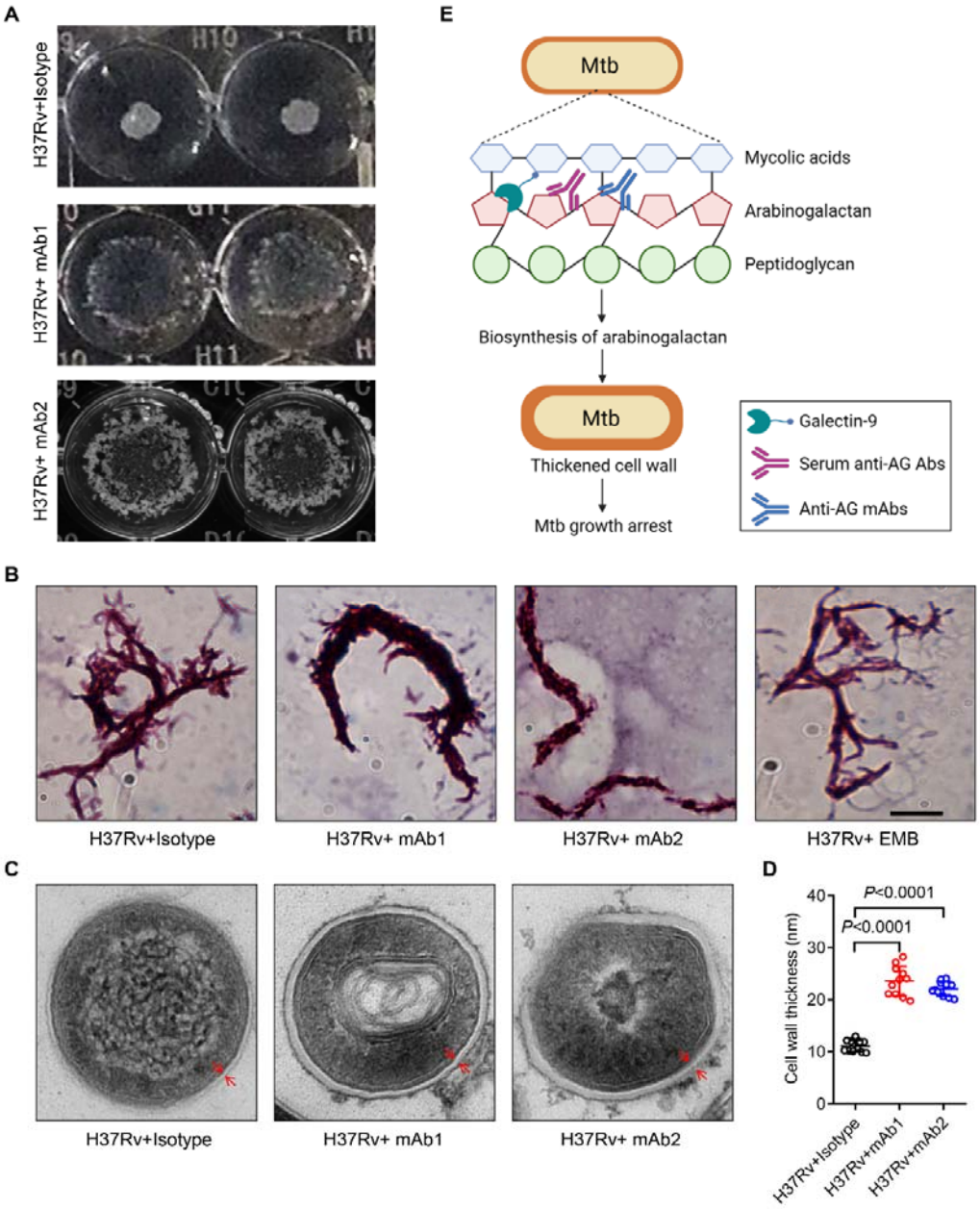

Figure 7. Mtb cell wall modulation by anti-AG antibodies.

A. Morphologic characteristics for Mtb H37Rv strain grown in liquid culture with or without anti-AG mAbs (1 μg/mL) observed by ×□2 magnifier.

B. Bacterial shape of Mtb H37Rv strain treated as in (A) observed by acid fast staining under a Leica DM2500 microscope using the 100× oil microscopy. EMB, Ethambutol. Scale bar, 20μm.

C. Ultrastructural morphology of Mtb H37Rv treated as in (A) analyzed by transmission electron microscopy (TEM). The cell wall was labeled with red arrows.

D. Cell wall thickness of bacteria in (C).

E. Schematic presentation of Mtb growth arrest by Galectin-9 or anti-AG antibodies.

Data are representative of three independent experiments with similar results (A, B and C). Data are means ± SD of 11 bacteria, representatives of three independent experiments (D). Two-tailed unpaired Student's t test (D). $P < 0.05$ was considered statistically significant.

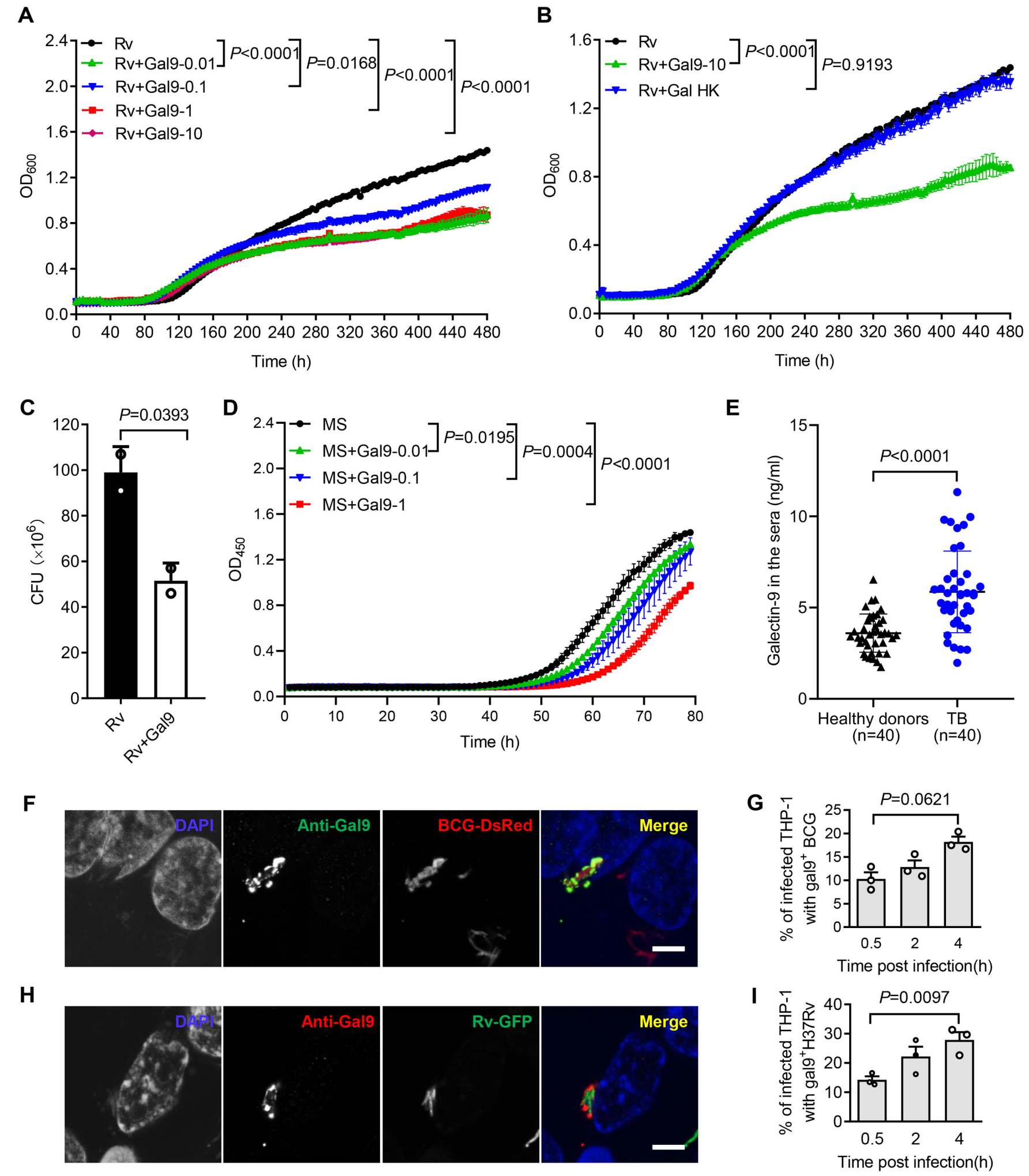
A
Rv
Rv+Gal9-0.01
Rv+Gal9-0.1
Rv+Gal9-1
Rv+Gal9-10
P<0.0001
P=0.0168
P<0.0001
P<0.0001
OD600
Time (h)
B
Rv
Rv+Gal9-10
Rv+Gal HK
P<0.0001
P=0.9193
OD600
Time (h)
C
P=0.0393
CFU (×10^6)
Rv
Rv+Gal9
D
MS
MS+Gal9-0.01
MS+Gal9-0.1
MS+Gal9-1
P=0.0195
P=0.0004
P<0.0001
OD450
Time (h)
E
P<0.0001
Galectin-9 in the sera (ng/ml)
Healthy donors (n=40)
TB (n=40)
F
DAPI
Anti-Gal9
BCG-DsRed
Merge
G
P=0.0621
% of infected THP-1 with gal9+ BCG
Time post infection(h)
H
DAPI
Anti-Gal9
Rv-GFP
Merge
I
P=0.0097
% of infected THP-1 with gal9+H37Rv
Time post infection(h)

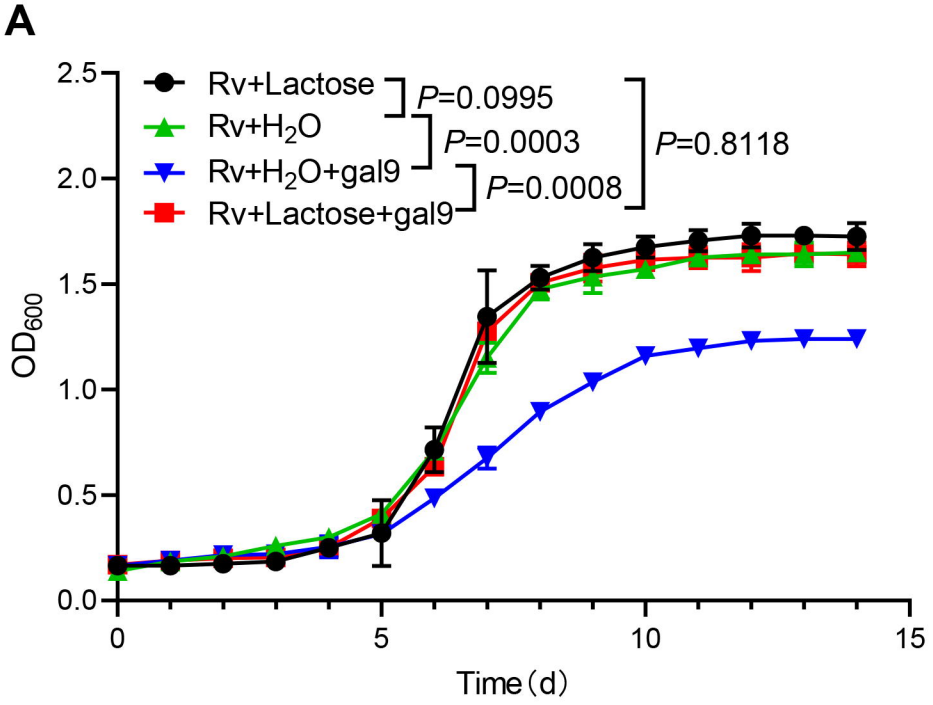
A
Rv+Lactose
Rv+H2O
Rv+H2O+gal9
Rv+Lactose+gal9
P=0.0995
P=0.0003
P=0.0008
P=0.8118
OD600
Time (d)

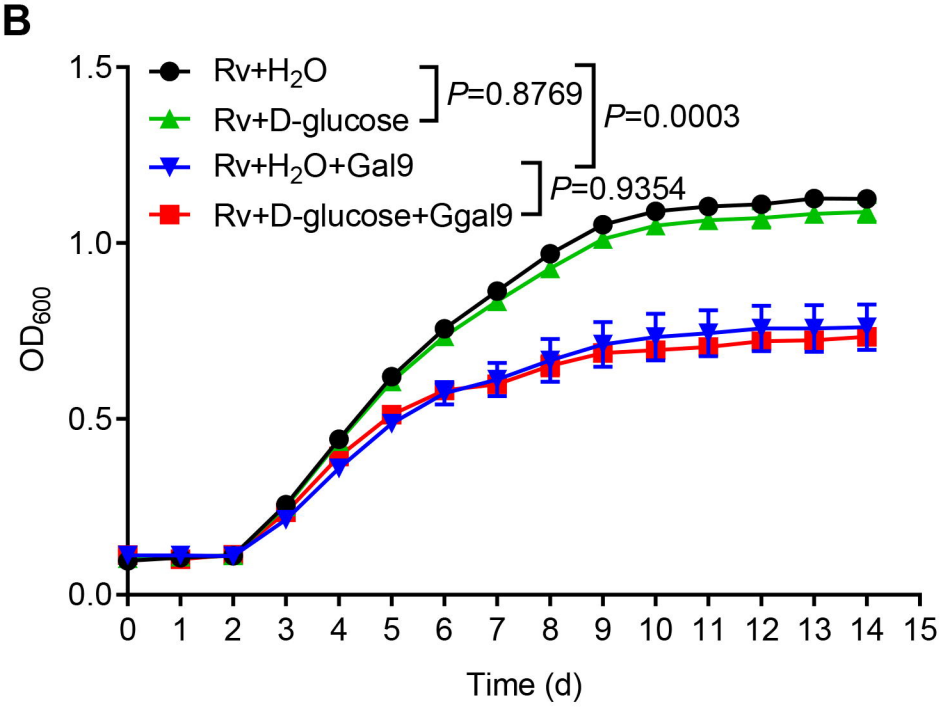
B
Rv+H2O
Rv+D-glucose
Rv+H2O+Gal9
Rv+D-glucose+Ggal9
P=0.8769
P=0.0003
P=0.9354
OD600
Time (d)

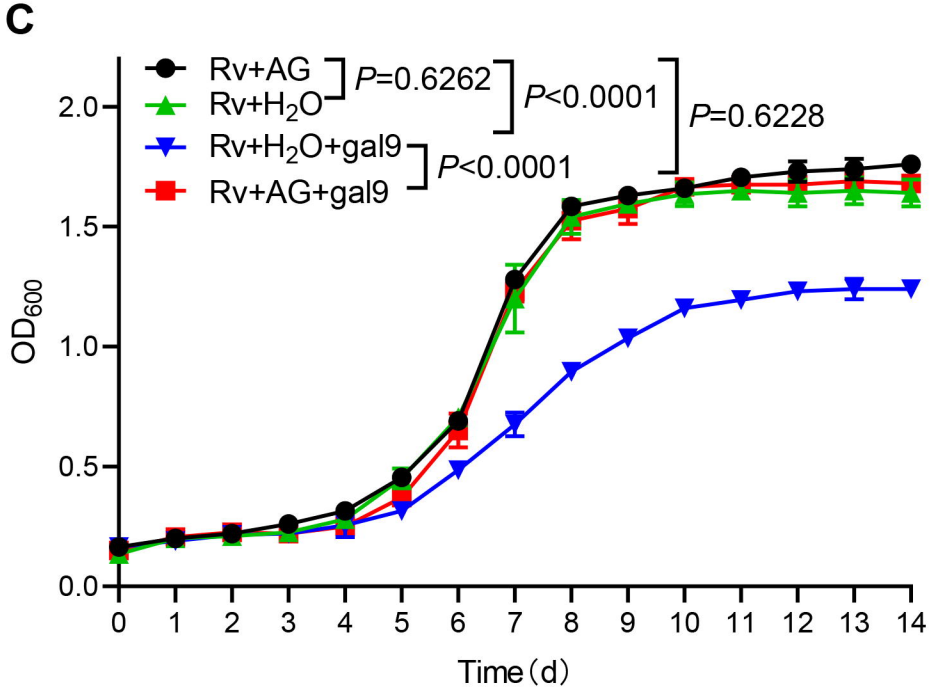
C
Rv+AG
Rv+H2O
Rv+H2O+gal9
Rv+AG+gal9
P=0.6262
P<0.0001
P<0.0001
P=0.6228
OD600
Time (d)

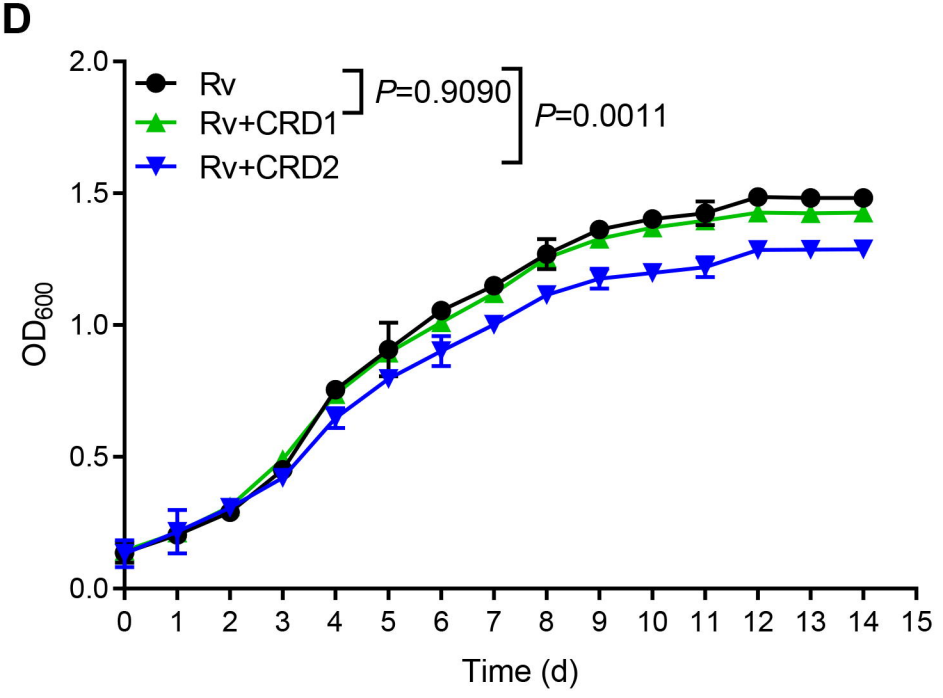
D
Rv
Rv+CRD1
Rv+CRD2
P=0.9090
P=0.0011
OD600
Time (d)

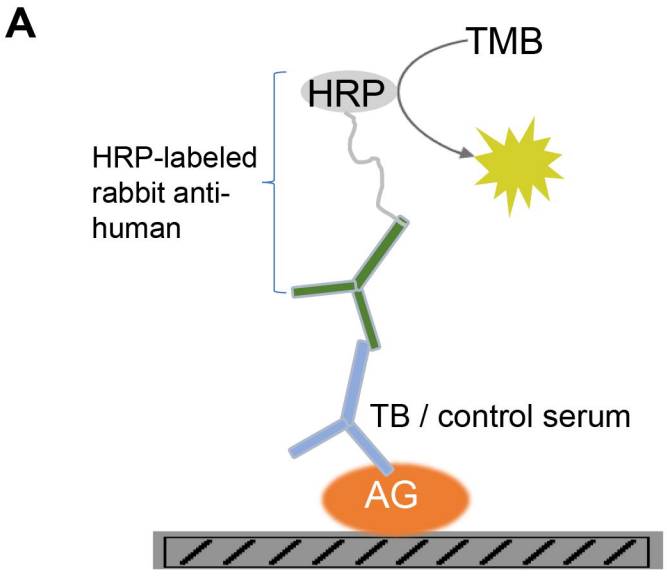
A
TMB
HRP
HRP-labeled
rabbit anti-
human
TB / control serum
AG

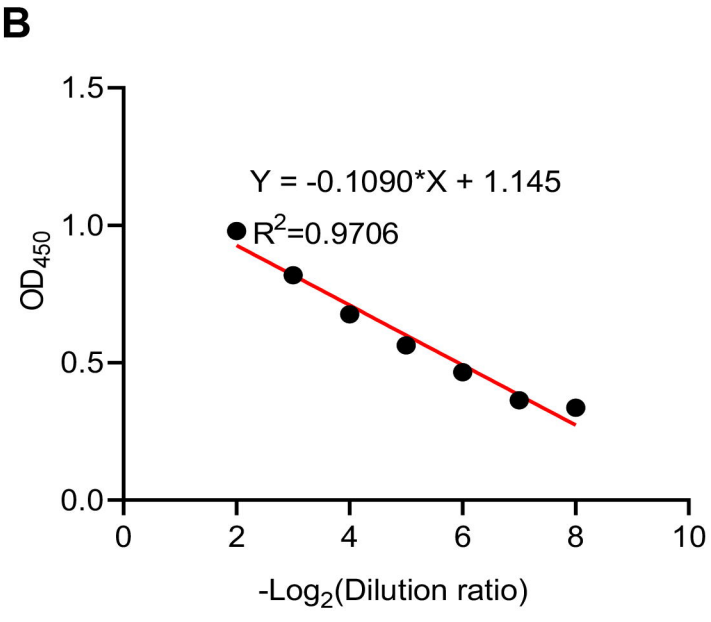
B
Y = -0.1090*X + 1.145
R2=0.9706
OD450
1.5
1.0
0.5
0.0
0
2
4
6
8
10
-Log2(Dilution ratio)

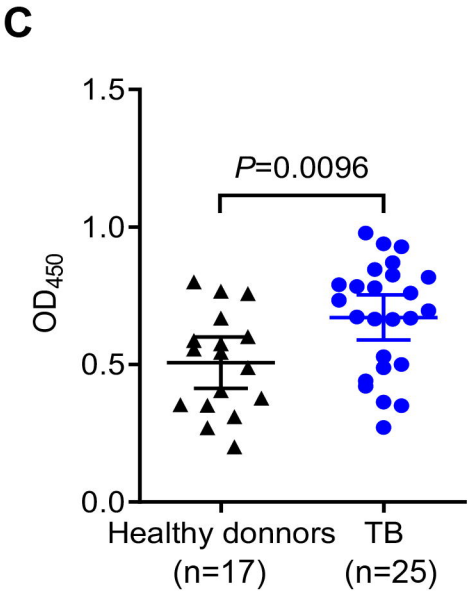
C
P=0.0096
OD450
1.5
1.0
0.5
0.0
Healthy donnors
(n=17)
TB
(n=25)

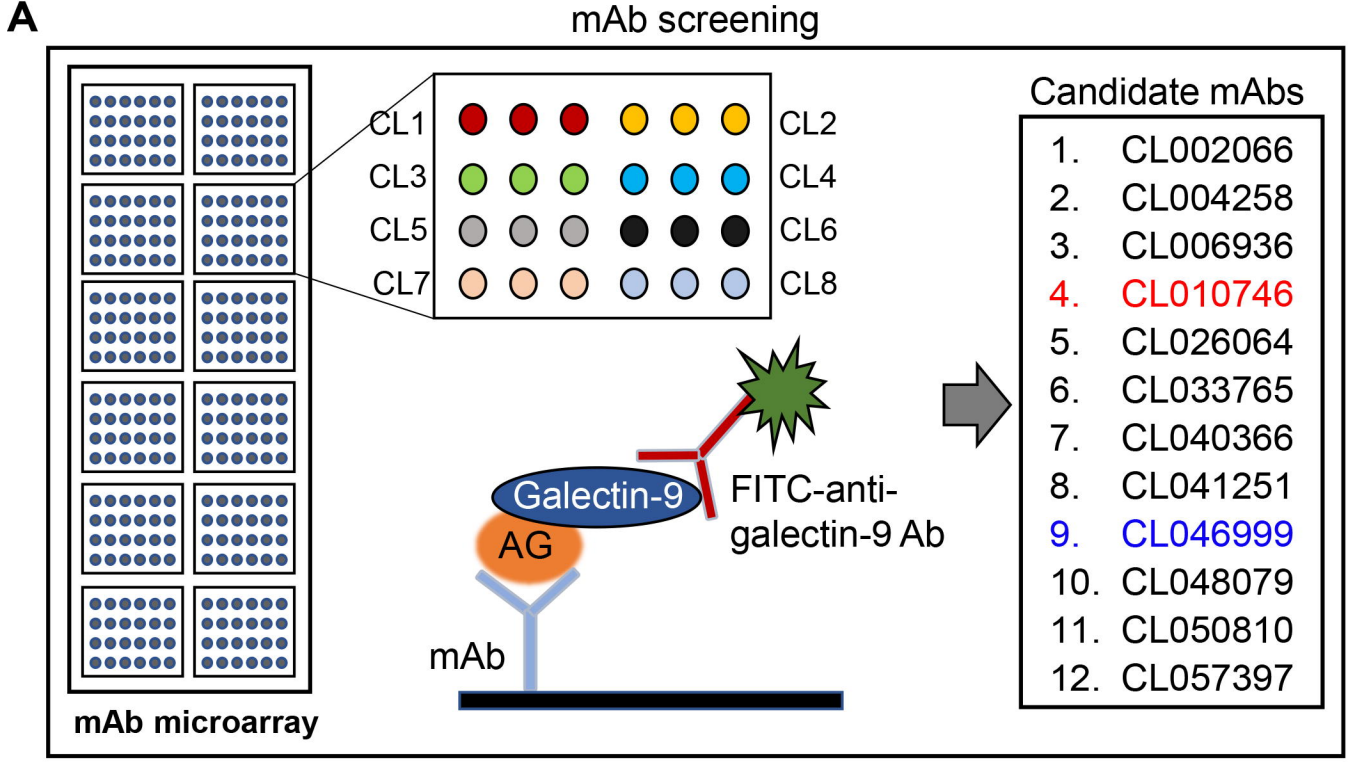
A
mAb screening
CL1
CL2
CL3
CL4
CL5
CL6
CL7
CL8
Galectin-9
AG
mAb
FITC-anti-galectin-9 Ab
mAb microarray
Candidate mAbs
1. CL002066
2. CL004258
3. CL006936
4. CL010746
5. CL026064
6. CL033765
7. CL040366
8. CL041251
9. CL046999
10. CL048079
11. CL050810
12. CL057397

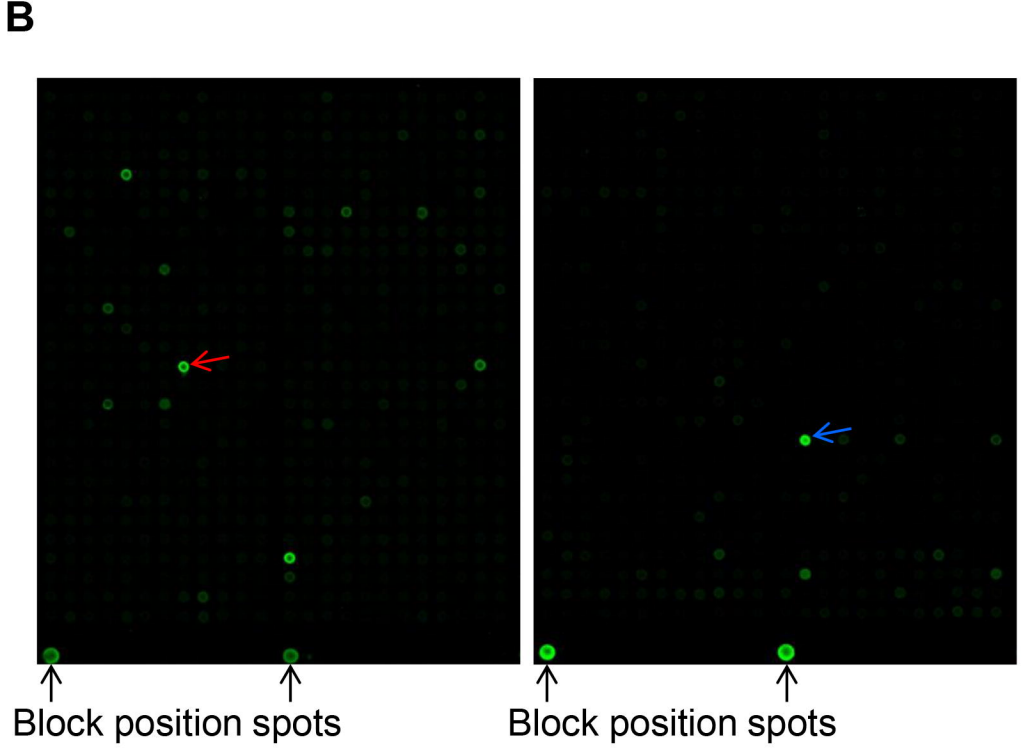
B
Block position spots
Block position spots

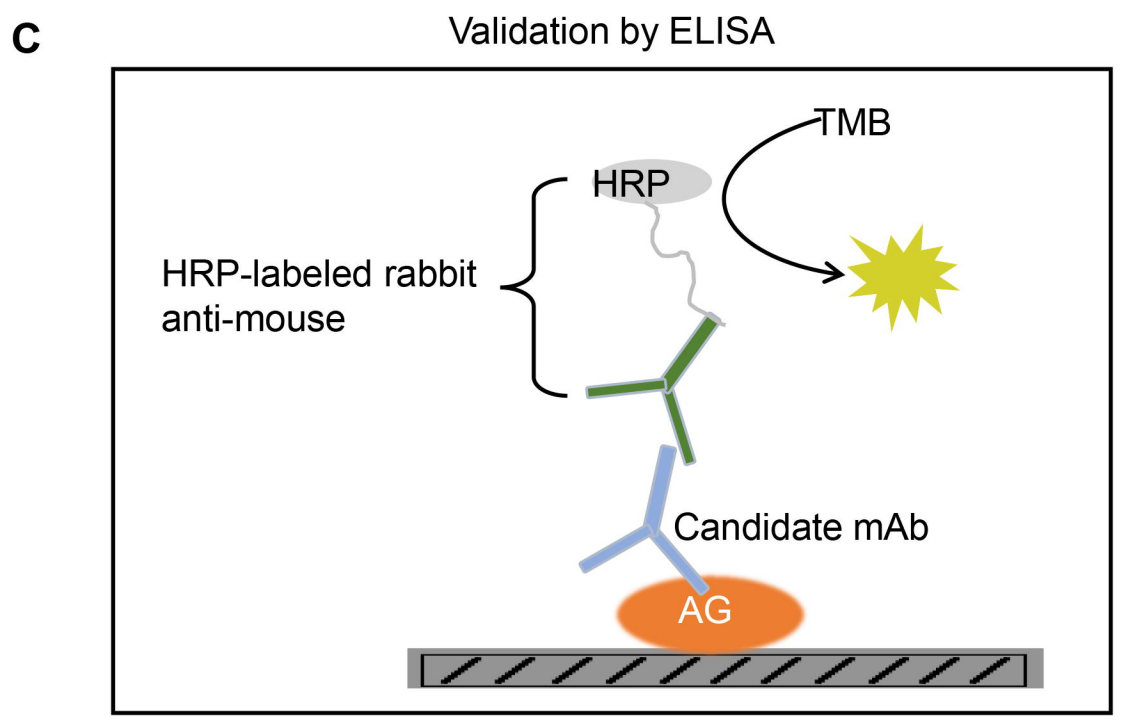
C
Validation by ELISA
TMB
HRP
HRP-labeled rabbit anti-mouse
Candidate mAb
AG

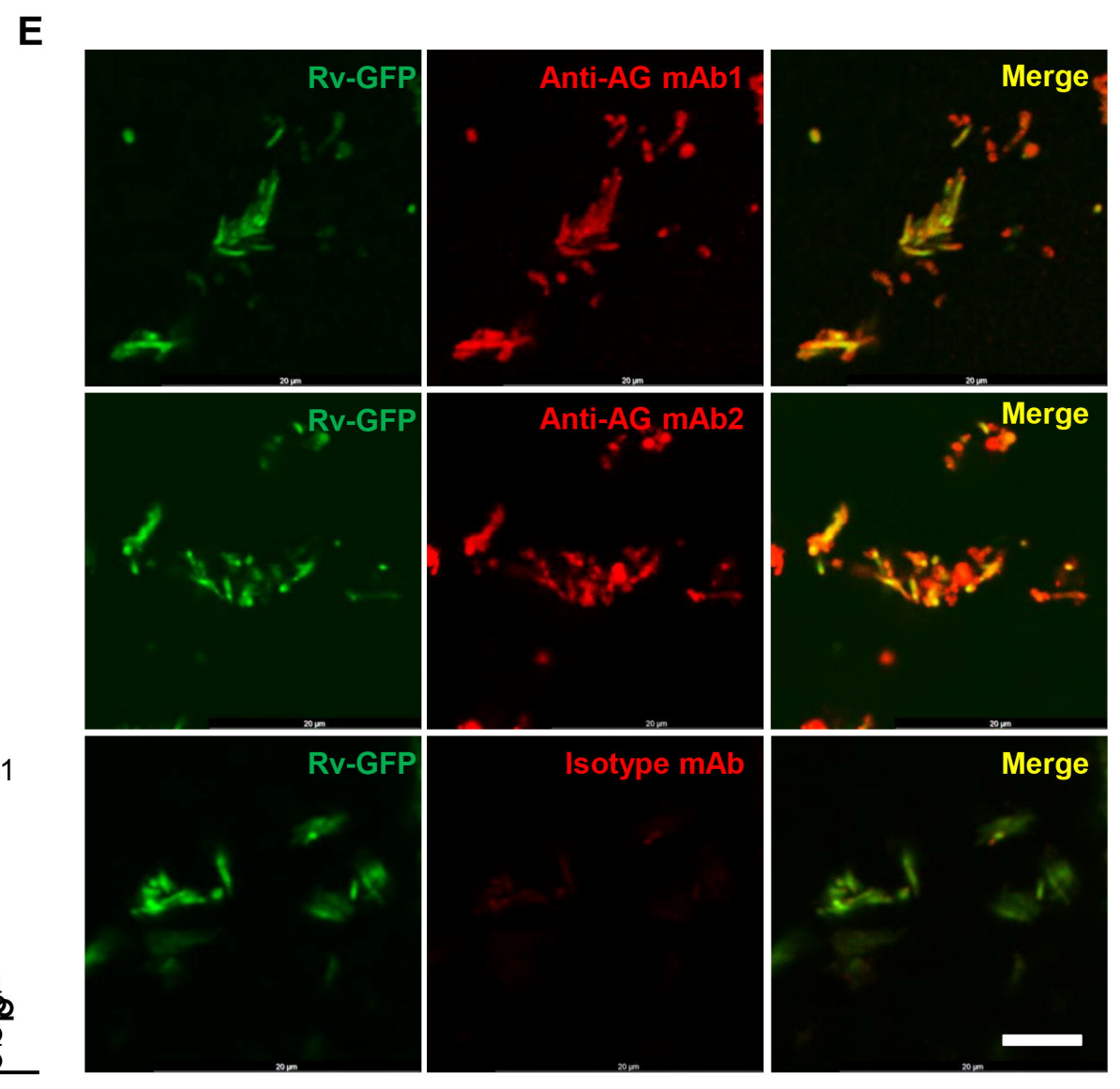
E
Rv-GFP
Anti-AG mAb1
Merge
Rv-GFP
Anti-AG mAb2
Merge
Rv-GFP
Isotype mAb
Merge

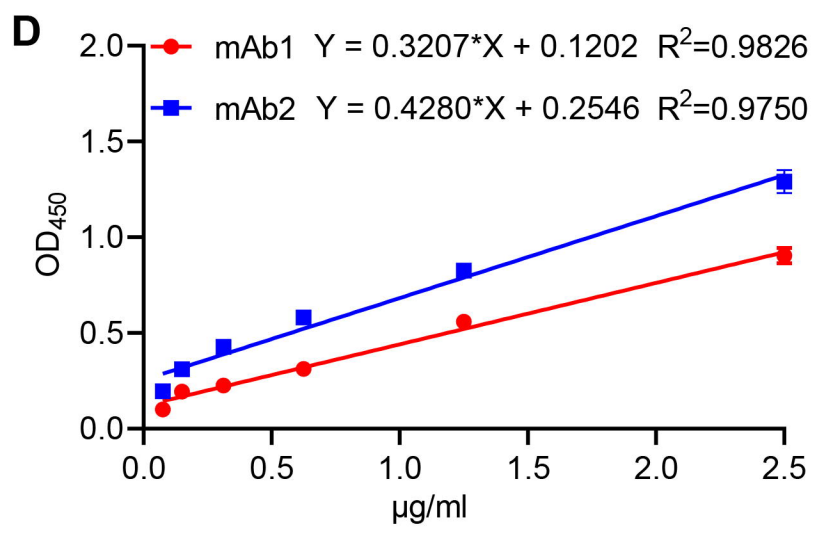
D
mAb1 Y = 0.3207*X + 0.1202 R2=0.9826
mAb2 Y = 0.4280*X + 0.2546 R2=0.9750
OD450
μg/ml
0.0
0.5
1.0
1.5
2.0
2.5

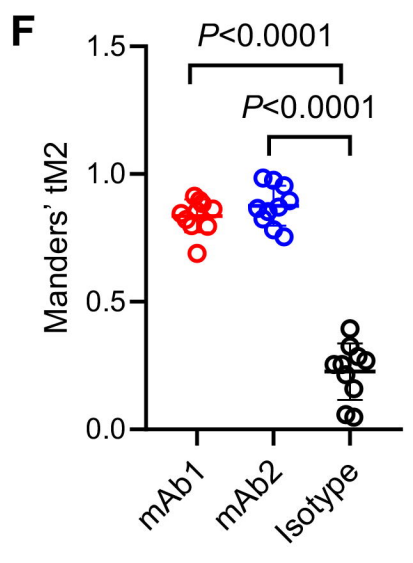
F
P<0.0001
P<0.0001
Manders' tM2
mAb1
mAb2
Isotype

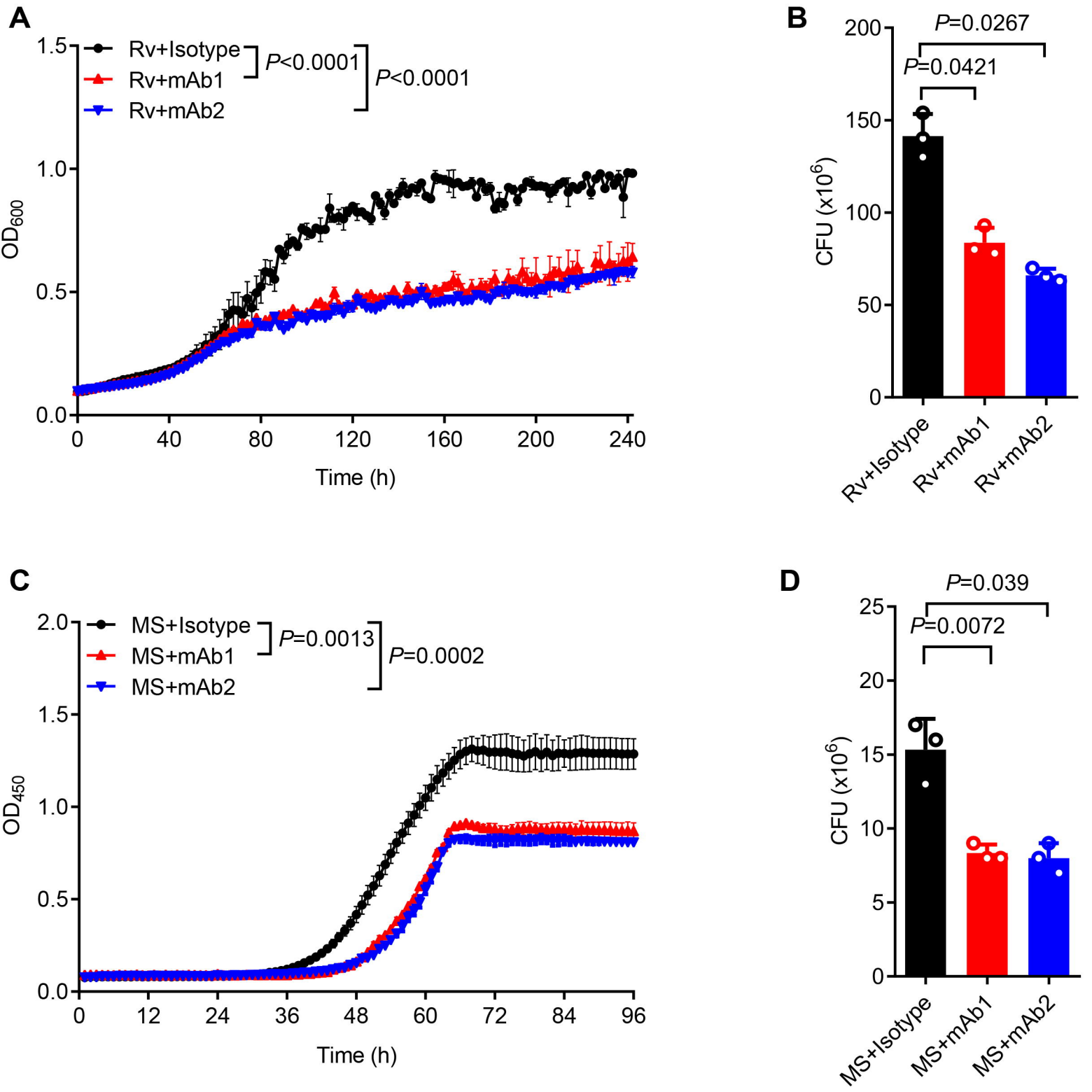
A
Rv+Isotype
Rv+mAb1
Rv+mAb2
P<0.0001
P<0.0001
OD600
Time (h)
B
P=0.0267
P=0.0421
CFU (x10^6)
Rv+Isotype
Rv+mAb1
Rv+mAb2
C
MS+Isotype
MS+mAb1
MS+mAb2
P=0.0013
P=0.0002
OD450
Time (h)
D
P=0.039
P=0.0072
CFU (x10^6)
MS+Isotype
MS+mAb1
MS+mAb2

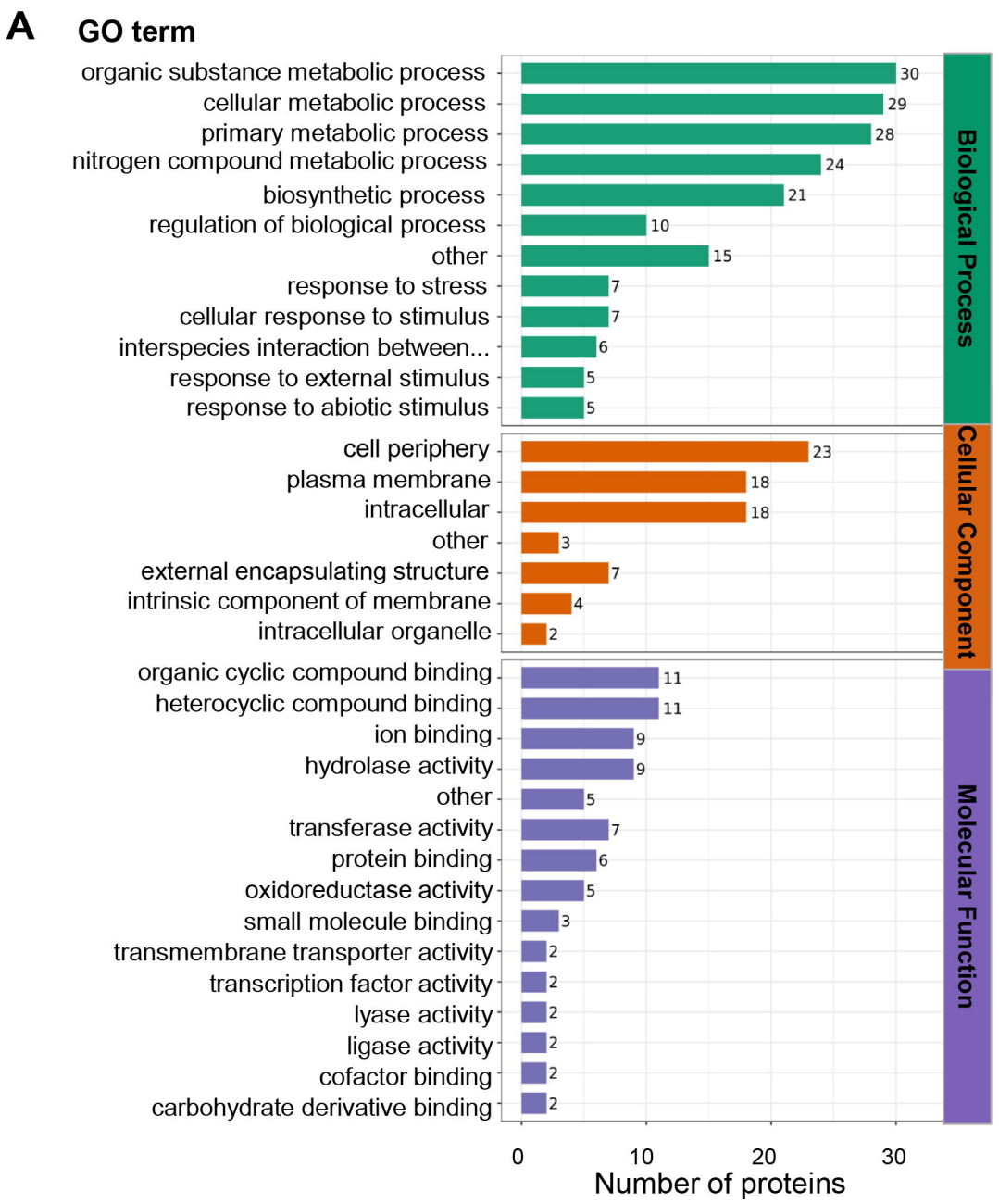

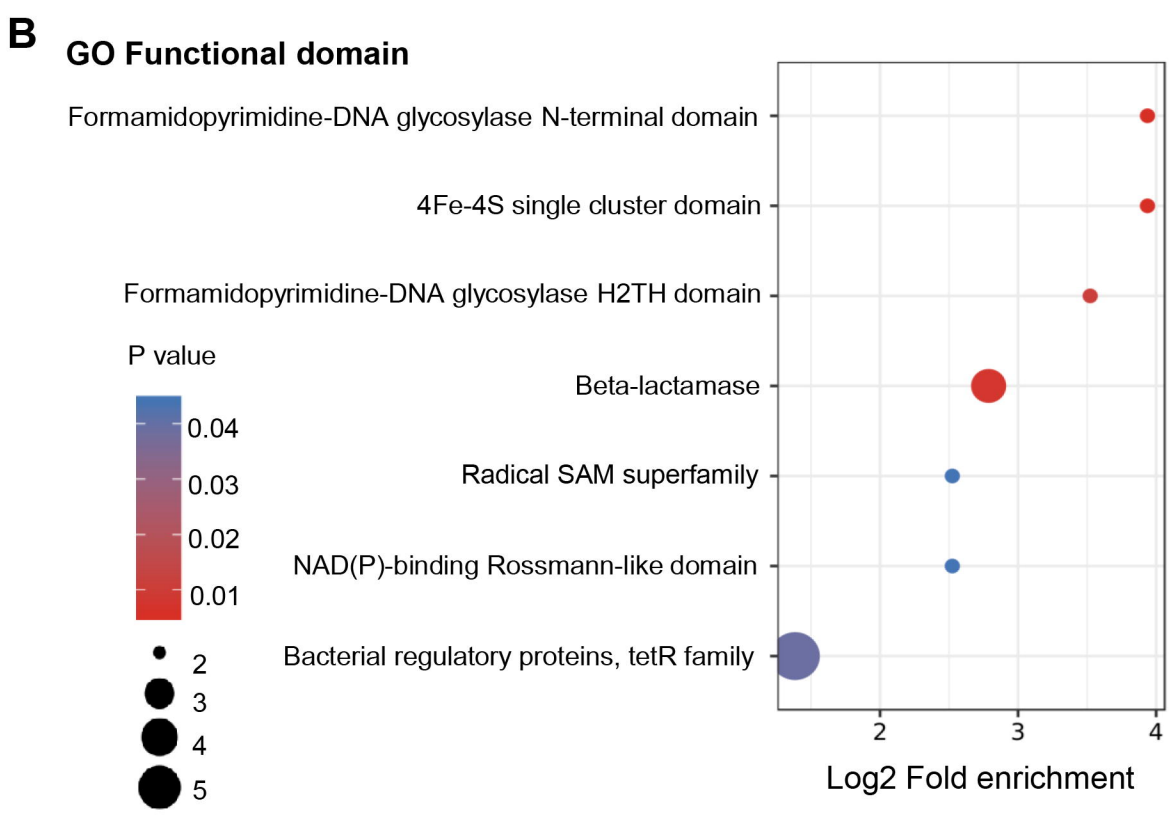

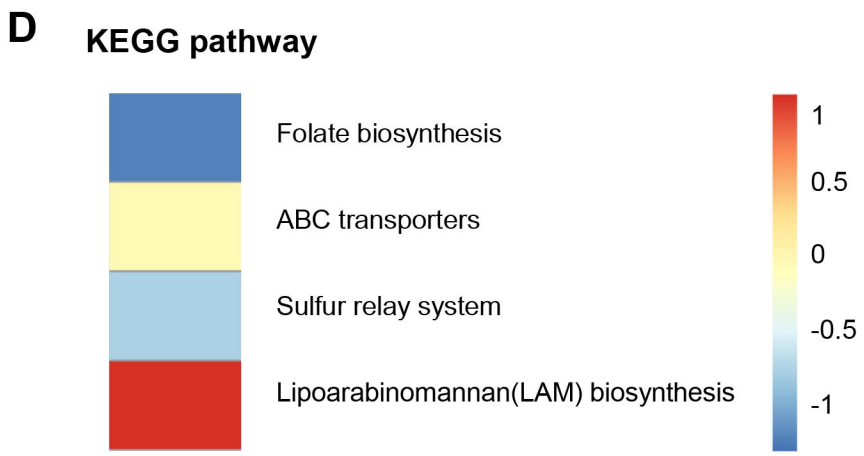

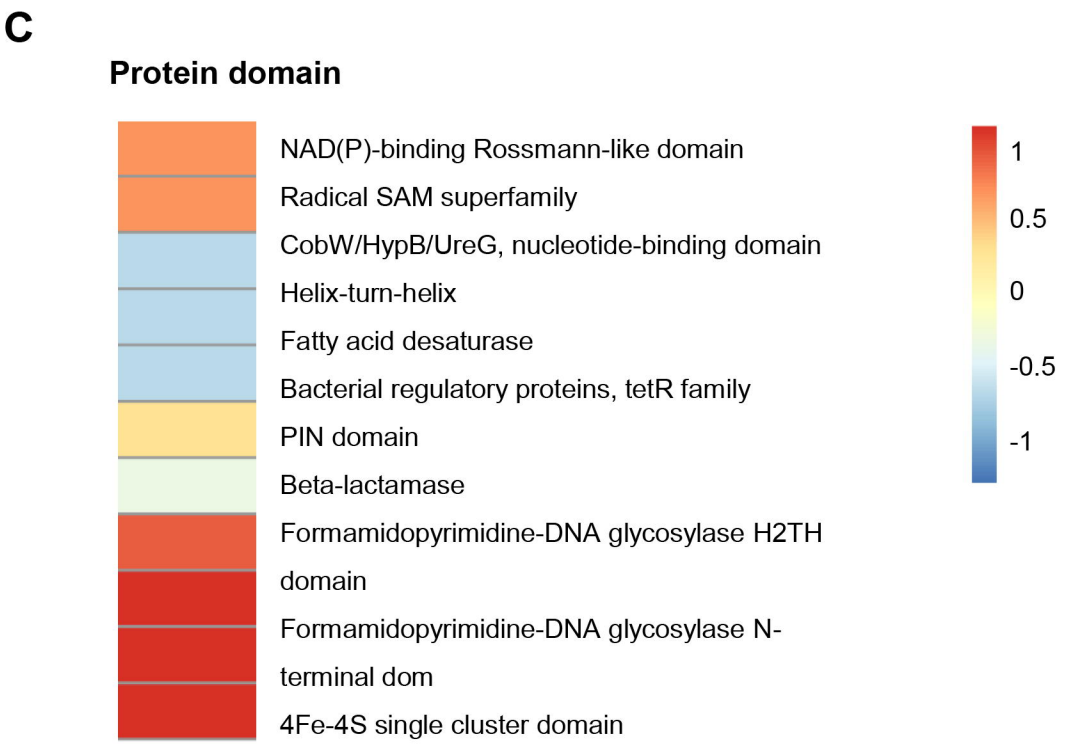

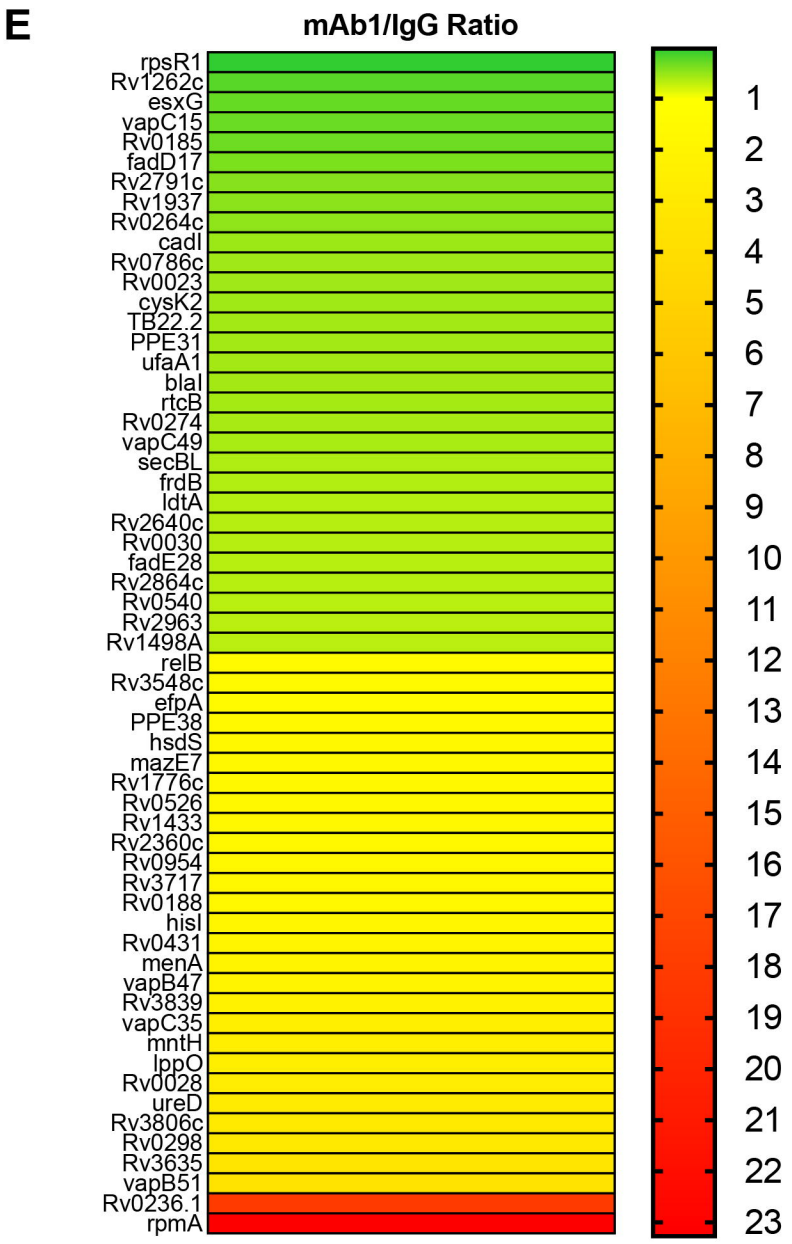

Locus	Name	Product	
Rv2441c	RpmA	50S ribosomal protein L27 RpmA	Involved in translation mechanisms
Rv0236c	aftD	Possible arabinofuranosyltransferase	Involved in the biosynthesis of the mycobacterial cell wall arabinan.
Rv0236A	Rv0236A	Small secreted protein	Cell wall and cell processes
Rv0229A	vapB51	antitoxin	Unknown
Rv3635		Probable conserved transmembrane protein	Unknown
Rv3806c	UbiA	Decaprenylphosphoryl-5-phosphoribose (DPPR) synthase	Involved in arabinogalactan synthesis

A

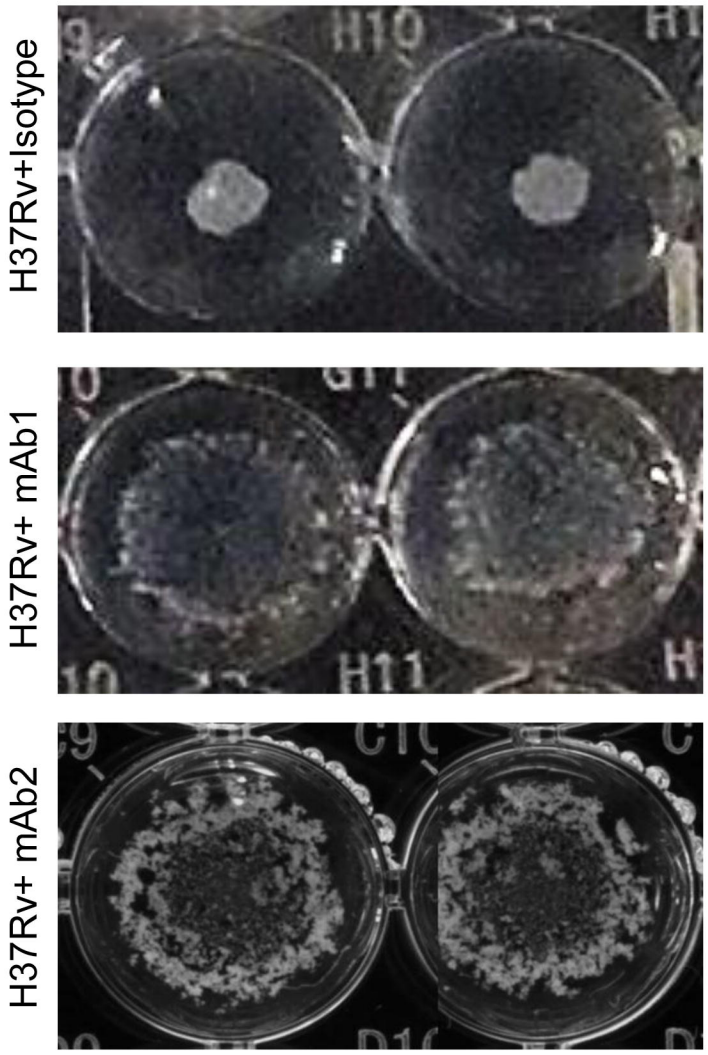
H37Rv+Isotype
H37Rv+ mAb1
H37Rv+ mAb2

E

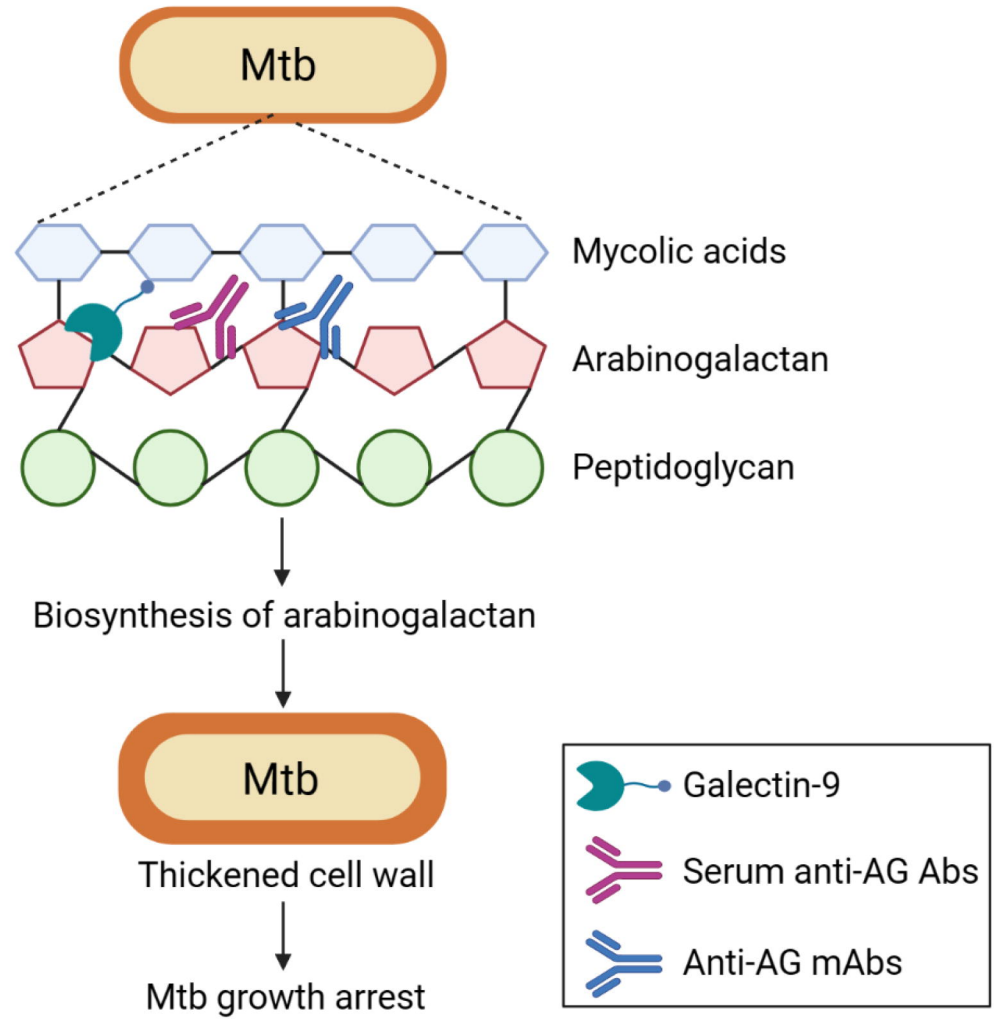
Mtb
Mycolic acids
Arabinogalactan
Peptidoglycan
Biosynthesis of arabinogalactan
Mtb
Thickened cell wall
Mtb growth arrest
Galectin-9
Serum anti-AG Abs
Anti-AG mAbs

B

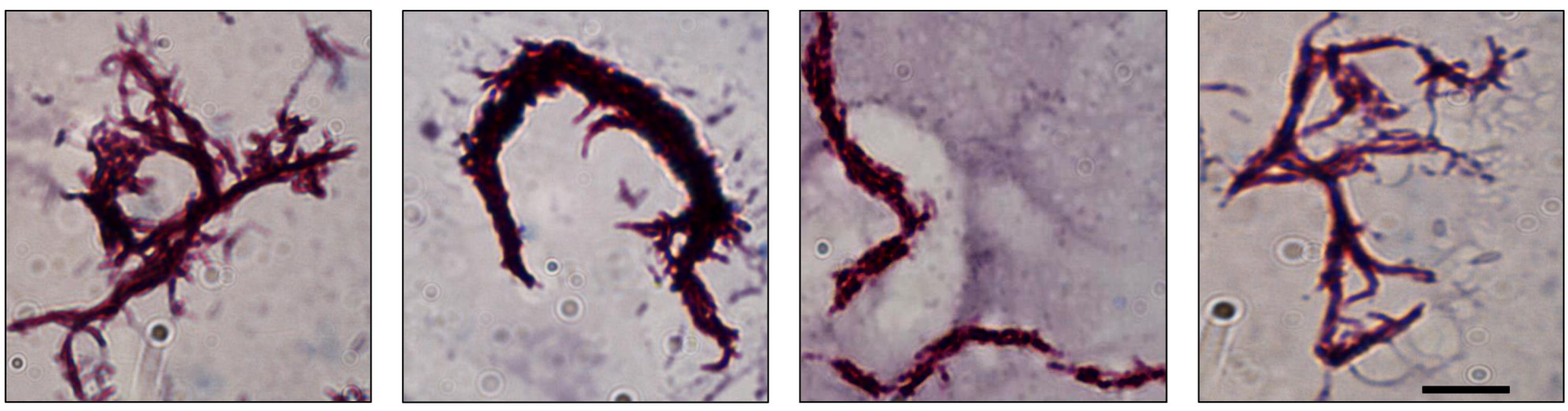
H37Rv+Isotype
H37Rv+ mAb1
H37Rv+ mAb2
H37Rv+ EMB

C

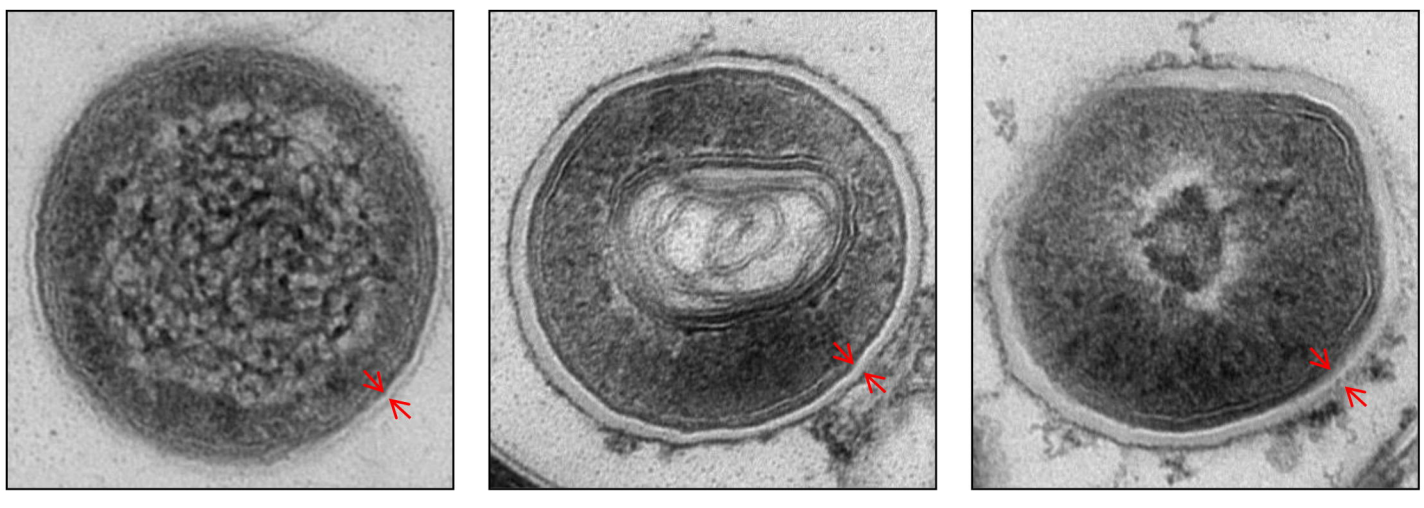
H37Rv+Isotype
H37Rv+ mAb1
H37Rv+ mAb2

D

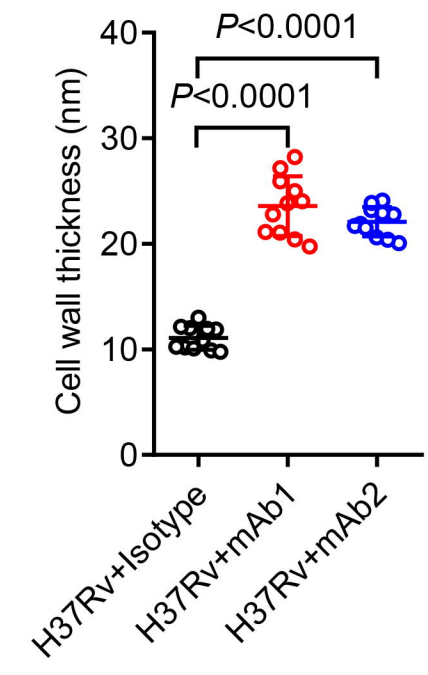
Cell wall thickness (nm)
40
30
20
10
0
P<0.0001
P<0.0001
H37Rv+Isotype
H37Rv+mAb1
H37Rv+mAb2